Signal Processing, vol. 83, 2003, pp. 1355–1378


ELSEVIER

Available at
www.ComputerScienceWeb.com
POWERED BY SCIENCE DIRECT®

Signal Processing 83 (2003) 1355–1378

SIGNAL PROCESSING

www.elsevier.com/locate/sigpro

# Wigner distributions (nearly) everywhere: time–frequency analysis of signals, systems, random processes, signal spaces, and frames☆

Gerald Matz*, Franz Hlawatsch

*Institute of Communications and Radio-Frequency Engineering, Vienna University of Technology, Gusshausstrasse 25/389, A-1040 Wien, Austria*

Received 16 December 2002

Dedicated to the Wigner distribution pioneer W. Mecklenbräuker on the occasion of his 65th birthday

**Abstract**

The Wigner distribution (WD) is perhaps the most prominent quadratic time–frequency signal representation. In this paper, which has mainly tutorial character but also contains some new results, we describe extensions of the WD concept to multidimensional vector signals, nonstationary random processes, linear time-varying systems (deterministic and random), linear signal spaces, and frames. We discuss the interpretation and properties of these WD extensions and various relations connecting them. Some application examples are also provided.


*Keywords:* Time–frequency analysis; Wigner distribution; Weyl symbol; Multidimensional vector signals; Nonstationary random processes; Linear time-varying systems; Linear signal spaces; Frames

## 1. Introduction

The *Wigner distribution* (WD) is perhaps the most prominent quadratic time–frequency (TF) representation. It was originally defined in a quantum mechanical context by Wigner in 1932 [66]. In 1948, Ville introduced the WD in a signal analysis context [64]. A mathematical analysis of the WD and the related *Weyl symbol* was provided by de Bruijn in 1973 [4]. However, it was not before the seminal three-part paper of Claasen and Mecklenbräuker [6–8] appeared in 1980 that the WD became widely popular in the signal processing community. In that paper, among other contributions, a comprehensive discussion of the signal-theoretic properties of the WD was given, a discrete-time WD and a windowed WD suitable for digital implementation were proposed, and the relation of the WD to other TF representations was discussed.

Since then, an impressive number of papers dealing with theoretical and practical aspects of the WD have been published; for references see e.g. [3,11,17,24,53,54]. The application areas for which the WD (or windowed/smoothed versions of the WD) have been proposed are as diverse as signal

☆ Funding by FWF Grant P15156.
* Corresponding author. Tel.: +43-1-58801-38916; fax: +43-1-58801-38999.
*E-mail addresses:* g.matz@ieee.org (G. Matz), fhlawats@pop.tuwien.ac.at (F. Hlawatsch).

0165-1684/03/$ - see front matter 
doi:10.1016/S0165-1684(03)00086-0

detection and enhancement, speech analysis, audio and acoustics, image processing and pattern analysis, biological and medical signal analysis, seismic prospecting, optics, machine diagnostics and fault detection, oceanography, radar imaging, source localization and separation, quantum mechanics, and mathematics.

In this paper, we demonstrate that the concept of the WD can be extended to several important mathematical objects beyond one-dimensional, scalar, deterministic signals. We describe extensions to multidimensional vector signals (Section 2), nonstationary random processes (Section 3), linear time-varying (LTV) systems (Section 4), random LTV systems (Section 5), linear signal spaces (Section 6), and frames (Section 7). Our paper has mainly tutorial or review character, although it contains some previously unpublished results. Special emphasis is placed on the properties of the various WD extensions and the relations connecting them. Some application examples are provided that demonstrate how specific characteristics of signals, systems, random processes, signal spaces, and frames can be inferred from the respective WD.

### 1.1. Wigner distribution

We first recall the original formulation of the WD of a scalar, one-dimensional (1-D) signal. For a continuous-time signal $x(t)$, the WD is defined as [1] [6]

$$W_x(t,f) \triangleq \int_\tau x\left(t+\frac{\tau}{2}\right) x^*\left(t-\frac{\tau}{2}\right) \mathrm{e}^{-\mathrm{j}2\pi f\tau}\,\mathrm{d}\tau. \quad (1)$$

The WD is a quadratic TF signal representation that can be loosely interpreted as an energy distribution over the TF plane. Such an interpretation cannot hold in a pointwise sense, however, since the uncertainty principle prohibits a pointwise TF localization of signals [10,17,20]. Due to its quadratic nature, the WD often contains cross terms (interference terms) whose geometry has been analyzed in detail in [25]. The WD cross terms partly assume large negative values (see [36] for a discussion of the positivity of bilinear TF signal representations). Nonetheless, it can be shown that

$$W_x(t,f) *_t *_f W_w(-t,-f) = |\langle x, w_{t,f}\rangle|^2 \geqslant 0. \quad (2)$$

Here, $w_{t,f}(t') = (\mathbf{S}_{t,f} w)(t') \triangleq w(t'-t)\mathrm{e}^{\mathrm{j}2\pi f t'}$, where $\mathbf{S}_{t,f}$ denotes the TF shift operator and $w(t)$ is a test signal that is assumed localized about the origin of the TF plane. According to (2), local averages of the WD (obtained by convolution with the WD of the test signal $w(t)$) are nonnegative and can be interpreted as the local energy of $x(t)$ about the TF analysis point $(t,f)$ (as measured by the inner product of $x$ with the TF shifted test signal $w_{t,f}(t')$).

The WD satisfies an impressive number of desirable mathematical properties. Several of these properties are listed in Table 1. The WD is a prominent member of the Cohen class of TF shift covariant TF representations [8,11,17,24]. All other Cohen class TF representations can be derived from the WD by means of a 2-D convolution.

The continuous-time form of the WD in (1) was later on complemented by the following definition for the WD of a discrete-time signal $x[n]$ [7]:

$$W_x(n,\theta) \triangleq 2\sum_{m=-\infty}^{\infty} x[n+m]x^*[n-m]\mathrm{e}^{-\mathrm{j}4\pi m\theta},$$

where $\theta$ denotes normalized frequency. Due to the factor of 4 in the exponent, this definition is applicable to so-called *halfband signals* whose Fourier transform occupies only a band of width $\frac{1}{2}$ (examples are analytic signals and signals that are oversampled by a factor of 2). Further results regarding discrete-time and also discrete–frequency WDs are provided e.g. in [9,56,58,61]. A formal extension of the WD to continuous groups has been proposed in [32].

**Example.** Among the many practical applications of the WD, we select a car engine diagnosis example for purposes of illustration. We consider high-pass filtered pressure signals that have been measured [2] in the combustion chamber of a car engine cylinder. Fig. 1 shows three different pressure signals and the corresponding WDs (a slight smoothing of the WD

[1] Integrals are from $-\infty$ to $\infty$.

[2] We are grateful to S. Carstens-Behrens, M. Wagner, and J.F. Böhme for providing us with the car engine data (courtesy of Aral-Forschung, Bochum).

Table 1
Some properties of the WD

| | |
|---|---|
| TF shift covariance | $\tilde{x}(t) = (\mathbf{S}_{t_0,f_0}x)(t) \Rightarrow W_{\tilde{x}}(t,f) = W_x(t-t_0, f-f_0)$ |
| Realvaluedness | $W_x(t,f) = W_x^*(t,f)$ |
| Marginal properties[a] | $\int_t W_x(t,f)\,\mathrm{d}t = \lvert X(f)\rvert^2$, $\int_f W_x(t,f)\,\mathrm{d}f = \lvert x(t)\rvert^2$ |
| Energy | $\int_t\int_f W_x(t,f)\,\mathrm{d}t\,\mathrm{d}f = \lVert x\rVert^2$, $\int_t\int_f W_x^2(t,f)\,\mathrm{d}t\,\mathrm{d}f = \lVert x\rVert^4$ |
| Moyal relation | $\int_t\int_f W_x(t,f)W_y(t,f)\,\mathrm{d}t\,\mathrm{d}f = \lvert\langle x,y\rangle\rvert^2$ |
| Finite support | $x(t)=0,\ t\notin[t_1,t_2] \Rightarrow W_x(t,f)=0,\ t\notin[t_1,t_2]$ |
| | $X(f)=0,\ f\notin[f_1,f_2] \Rightarrow W_x(t,f)=0,\ f\notin[f_1,f_2]$ |
| Symplectic covariance[b] | $\tilde{x}(t) = (\mu(\boldsymbol{A})x)(t) \Rightarrow W_{\tilde{x}}(t,f) = W_x(\boldsymbol{A}\binom{t}{f})$ |

[a] $X(f)$ denotes the Fourier transform of $x(t)$, i.e., $X(f) = \int_t x(t)\mathrm{e}^{-\mathrm{j}2\pi ft}\,\mathrm{d}t$.
[b] Here, $\mu(\boldsymbol{A})$ denotes the unitary operator associated to a $2\times 2$ unimodular matrix $\boldsymbol{A}$ via the metaplectic representation [19, Chapter 4]. Special cases of $\mu(\boldsymbol{A})$ include TF scaling, Fourier transform, chirp multiplication, and chirp convolution.

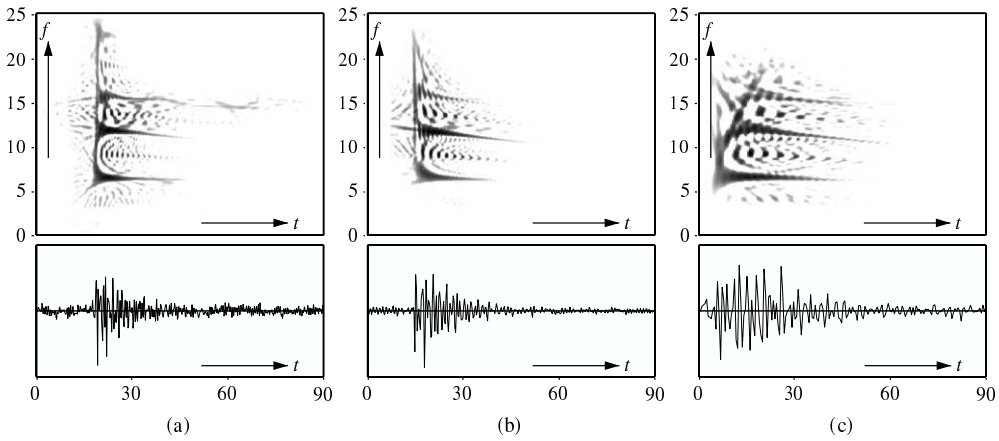


Fig. 1. WD (top) of pressure signals (bottom) measured in a car engine running at (a) 1000 rpm, (b) 2000 rpm, and (c) 4000 rpm. Only positive parts of the WD are shown, with darker shading corresponding to larger amplitudes. Horizontal axis: crank angle (which is proportional to time), vertical axis: frequency in kHz.

was used to increase readability while retaining some of the cross terms). The three pressure signals correspond to knocking combustions at engine speeds of 1000, 2000, and 4000 rpm, respectively. The WDs of these signals allow us to identify several resonant components with abrupt onsets and frequencies that decrease with time. (The decreasing frequencies can be explained by the decreasing temperature of the gas in the combustion chamber and by the movement of the piston [5,37].) Between the resonance components, the WDs feature large oscillating and partly negative cross terms. According to (2), these cross terms do not indicate local energetic contributions in the pressure signals (note, however, that the cross terms may manifest themselves e.g. in the WD marginals [25]). An attenuation of the cross terms can be achieved by

Table 2
Some properties of the WS

| | |
|---|---|
| TF shift covariance[a] | $\tilde{\mathbf{H}} = \mathbf{S}_{t_0,f_0}\mathbf{H}\mathbf{S}^{+}_{t_0,f_0} \Rightarrow L_{\tilde{\mathbf{H}}}(t,f) = L_{\mathbf{H}}(t-t_0, f-f_0)$ |
| Adjoint; realvaluedness | $L_{\mathbf{H}^+}(t,f) = L^*_{\mathbf{H}}(t,f)$; |
| | $\mathbf{H} = \mathbf{H}^+ \Rightarrow L_{\mathbf{H}}(t,f) = L^*_{\mathbf{H}}(t,f)$ |
| Marginal properties[b] | $\int_t L_{\mathbf{H}}(t,f)\,\mathrm{d}t = H(f,f)$, $\int_f L_{\mathbf{H}}(t,f)\,\mathrm{d}f = h(t,t)$ |
| Trace | $\int_t\int_f L_{\mathbf{H}}(t,f)\,\mathrm{d}t\,\mathrm{d}f = \mathrm{tr}\{\mathbf{H}\} = \int_t h(t,t)\,\mathrm{d}t$ |
| Energy | $\int_t\int_f \lvert L_{\mathbf{H}}(t,f)\rvert^2\,\mathrm{d}t\,\mathrm{d}f = \lVert\mathbf{H}\rVert^2 = \int_t\int_{t'} \lvert h(t,t')\rvert^2\,\mathrm{d}t\,\mathrm{d}t'$ |
| Moyal-type relation | $\int_t\int_f L_{\mathbf{H}_1}(t,f)L^*_{\mathbf{H}_2}(t,f)\,\mathrm{d}t\,\mathrm{d}f = \langle\mathbf{H}_1,\mathbf{H}_2\rangle$ |
| | $= \int_t\int_{t'} h_1(t,t')h_2^*(t,t')\,\mathrm{d}t\,\mathrm{d}t'$ |
| Finite support | $h^{(\mathrm{s})}(t,\tau) = 0,\ t\notin[t_1,t_2] \Rightarrow L_{\mathbf{H}}(t,f) = 0,\ t\notin[t_1,t_2]$ |
| | $H^{(\mathrm{s})}(f,\nu) = 0,\ f\notin[f_1,f_2] \Rightarrow L_{\mathbf{H}}(t,f) = 0,\ f\notin[f_1,f_2]$ |
| Symplectic covariance | $\tilde{\mathbf{H}} = \mu(\boldsymbol{A})\mathbf{H}\mu(\boldsymbol{A})^+ \Rightarrow L_{\tilde{\mathbf{H}}}(t,f) = L_{\mathbf{H}}(\boldsymbol{A}\left(\begin{smallmatrix}t\\f\end{smallmatrix}\right))$ |

[a] The superscript $^+$ is used to denote the adjoint [55] of an operator.
[b] $H(f,f')$ and $H^{(\mathrm{s})}(f,\nu) = H(f+\frac{\nu}{2}, f-\frac{\nu}{2})$ denote the 2-D Fourier transforms of $h(t,t')$ and $h^{(\mathrm{s})}(t,\tau)$, respectively.

means of a stronger smoothing, which would however result in a loss of TF resolution.

### 1.2. Weyl symbol

We next discuss the *Weyl symbol* (WS), which is a linear TF representation of a linear operator that is closely related to the WD. The WS also has its origins in quantum mechanics (cf. [4,19,65,67]) and was later used in mathematics as a "symbol" for pseudo-differential operators [19,33,67]. It was introduced in signal processing as a means for characterizing linear time-varying (LTV) systems/filters and TF localization operators [13,38,40,47,59,63].

Consider a linear operator[3] (LTV system) $\mathbf{H}$ with kernel (impulse response) $h(t,t')$ and input–output relation

$$y(t) = (\mathbf{H}x)(t) = \int_{t'} h(t,t')x(t')\,\mathrm{d}t'.$$

The WS of the operator $\mathbf{H}$ is defined as [13,38,40,47,59,63]

$$L_{\mathbf{H}}(t,f) \triangleq \int_\tau h\left(t+\frac{\tau}{2}, t-\frac{\tau}{2}\right)\mathrm{e}^{-\mathrm{j}2\pi f\tau}\,\mathrm{d}\tau = \int_\tau h^{(\mathrm{s})}(t,\tau)\mathrm{e}^{-\mathrm{j}2\pi f\tau}\,\mathrm{d}\tau, \tag{3}$$

where $h^{(\mathrm{s})}(t,\tau) \triangleq h(t+\frac{\tau}{2}, t-\frac{\tau}{2})$. The WS is a linear representation of $\mathbf{H}$. The kernel of $\mathbf{H}$ can be reobtained from the WS via

$$h(t,t') = \int_f L_{\mathbf{H}}\left(\frac{t+t'}{2}, f\right)\mathrm{e}^{\mathrm{j}2\pi f(t-t')}\,\mathrm{d}f, \tag{4}$$

which shows that the WS contains all information about $\mathbf{H}$. Further important mathematical properties of the WS are summarized in Table 2.

Comparison of (3) and (1) shows that the WD is equal to the WS of the rank-one operator $x\otimes x^*$ whose

[3] Linear operators (linear systems), matrices, and vectors are denoted by boldface letters. We use upright capital letters for operators, italic capital letters for matrices, and italic lowercase letters for vectors.

kernel equals $x(t)x^*(t')$, i.e.,

$$W_x(t,f) = L_{x\otimes x^*}(t,f).$$

Another important relation of the WS and WD pertains to quadratic forms:

$$\langle \mathbf{H}x, x\rangle = \langle L_{\mathbf{H}}, W_x\rangle = \int_t \int_f L_{\mathbf{H}}(t,f) W_x(t,f)\,\mathrm{d}t\,\mathrm{d}f$$

(note that there is no conjugation of $W_x(t,f)$ in the last expression since the WD is real-valued). Hence, quadratic forms induced by an operator $\mathbf{H}$ can be reformulated in the TF domain with the WS $L_{\mathbf{H}}(t,f)$ as TF representation of $\mathbf{H}$ and the WD $W_x(t,f)$ as the associated TF signal representation. Using this property, it follows that

$$L_{\mathbf{H}}(t,f) *_t *_f W_w(-t,-f) = \langle \mathbf{H} w_{t,f}, w_{t,f}\rangle.$$

This means that a local average of the WS (obtained by convolution with the WD of a suitable test signal $w(t)$) is a measure of the gain (amplification/attenuation) of $\mathbf{H}$ about the TF analysis point $(t,f)$. Yet another relation between the WS and WD is obtained for systems with an eigenvalue decomposition of the form $\mathbf{H}=\sum_{k=1}^{\infty} \lambda_k u_k \otimes u_k^*$. Here, the WS is given by

$$L_{\mathbf{H}}(t,f) = \sum_{k=1}^{\infty} \lambda_k W_{u_k}(t,f),$$

i.e., the WS of $\mathbf{H}$ is a weighted superposition of WDs.

In the practically important case of *underspread* LTV systems (i.e., LTV systems that introduce TF shifts only with small time and frequency lags), the WS constitutes an approximate TF transfer function with properties that are analogous to those of the ordinary transfer function of LTI systems [40,47]. This TF transfer function interpretation enables the design of LTV filters based on the WS [38,51] and the use of the WS in statistical signal processing (nonstationary signal estimation and detection) [28,30,31,46,49,62].

A transfer function interpretation of the WS is no longer valid for *overspread* LTV systems that introduce significant TF shifts. These TF shifts are reflected in the WS by oscillating "interference" terms that prohibit an interpretation of the WS as TF transfer function. In the overspread case, the input WD, output WD, and transfer WD discussed in Section 4 typically yield more useful insights than the WS. An interpretation of the interference terms of the WS is provided by the relation

$$\int_\tau \int_\nu \widetilde{\mathscr{W}}_{\mathbf{H}}(t,f;\tau,\nu)\,\mathrm{d}\tau\,\mathrm{d}\nu = |L_{\mathbf{H}}(t,f)|^2. \tag{5}$$

Here, $\widetilde{\mathscr{W}}_{\mathbf{H}}(t,f;\tau,\nu)$ denotes the transfer WD of $\mathbf{H}$ (cf. Section 4) that describes the energy transfer from the TF point $(t-\tau/2, f-\nu/2)$ to the TF point $(t+\tau/2, f+\nu/2)$ effected by $\mathbf{H}$. Consequently, (5) shows that large values of $L_{\mathbf{H}}(t,f)$ at a specific TF analysis point $(t,f)$ do not necessarily indicate a large system gain at $(t,f)$ but may also be due to a large energy transfer effected by $\mathbf{H}$ between TF points located symmetrically about $(t,f)$.

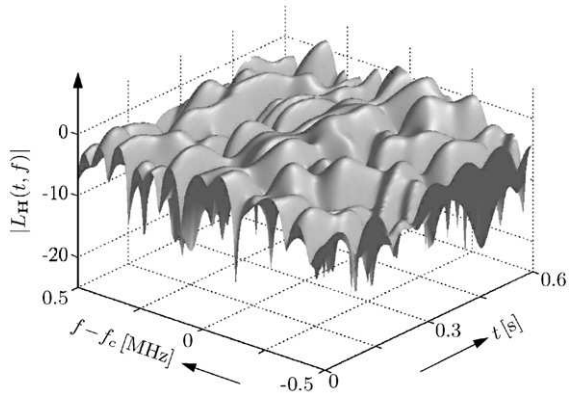


Fig. 2. WS magnitude (in dB) of a measured mobile radio channel.

**Example.** To illustrate the application of the WS, we consider an example where the LTV system under analysis is a mobile radio channel measured[4] in a suburban environment. Fig. 2 shows the WS of this channel over a time interval of length 600 ms and a frequency band of width 1 MHz and center frequency $f_c = 1.792$ GHz. The time- and frequency-varying attenuation of the channel is clearly displayed. In particular, several deep fades at various TF points are recognizable. We note that this mobile radio channel

[4] The measurements were performed in the course of the METAMORP project [34]. We are grateful to T-NOVA Deutsche Telekom Innovationsgesellschaft mbH (Technologiezentrum Darmstadt, Germany) and to I. Gaspard and M. Steinbauer for providing us with the measurement data.

is underspread and thus its WS can indeed be interpreted as a TF transfer function.

## 2. Multidimensional vector signals

In this section, we will extend the WD and WS to multidimensional vector signals and the associated operators. In a mathematical context, definitions of a multidimensional WD and WS were provided in [19]. Furthermore, the WD of a vector signal that is a function of a single variable has been used in a signal processing context e.g. in [68]. Here, we extend this previous work by defining and studying multidimensional matrix-valued WD and WS.

### 2.1. Wigner distribution

The WD of a $D$-dimensional, length-$K$ signal vector $\boldsymbol{x}(\boldsymbol{t}) = [x_1(t_1,\ldots,t_D)\ldots x_K(t_1,\ldots,t_D)]^{\mathrm{T}}$ is defined as

$$\boldsymbol{W}_{\boldsymbol{x}}(\boldsymbol{t},\boldsymbol{f}) \triangleq \int_{\boldsymbol{\tau}} \boldsymbol{x}\left(\boldsymbol{t}+\frac{\boldsymbol{\tau}}{2}\right) \times \boldsymbol{x}^{\mathrm{H}}\left(\boldsymbol{t}-\frac{\boldsymbol{\tau}}{2}\right) \mathrm{e}^{-\mathrm{j}2\pi \boldsymbol{f}^{\mathrm{T}}\boldsymbol{\tau}}\,\mathrm{d}\boldsymbol{\tau}, \tag{6}$$

where $\boldsymbol{t} = [t_1\ldots t_D]^{\mathrm{T}}$, $\boldsymbol{f} = [f_1\ldots f_D]^{\mathrm{T}}$, and $\boldsymbol{\tau} = [\tau_1\ldots\tau_D]^{\mathrm{T}}$. Thus, the WD $\boldsymbol{W}_{\boldsymbol{x}}(\boldsymbol{t},\boldsymbol{f}) = [W_{x_k,x_l}(\boldsymbol{t},\boldsymbol{f})]$ is a $K\times K$ matrix with each entry $W_{x_k,x_l}(\boldsymbol{t},\boldsymbol{f}) = \int_{\boldsymbol{\tau}} x_k(\boldsymbol{t}+\frac{\boldsymbol{\tau}}{2})x_l^*(\boldsymbol{t}-\frac{\boldsymbol{\tau}}{2})\mathrm{e}^{-\mathrm{j}2\pi\boldsymbol{f}^{\mathrm{T}}\boldsymbol{\tau}}\,\mathrm{d}\boldsymbol{\tau}$ being a function of time $\boldsymbol{t}$ and frequency $\boldsymbol{f}$.

In the following, we discuss important mathematical properties of the above WD definition. These properties generalize the properties of the ordinary WD listed in Table 1.

*TF shift covariance*. The WD of the TF shifted signal $\tilde{\boldsymbol{x}}(\boldsymbol{t}) = (\mathbf{S}_{\boldsymbol{t}_0,\boldsymbol{f}_0}\boldsymbol{x})(\boldsymbol{t}) \triangleq \boldsymbol{x}(\boldsymbol{t}-\boldsymbol{t}_0)\mathrm{e}^{\mathrm{j}2\pi\boldsymbol{f}_0^{\mathrm{T}}\boldsymbol{t}}$ satisfies

$$\boldsymbol{W}_{\tilde{\boldsymbol{x}}}(\boldsymbol{t},\boldsymbol{f}) = \boldsymbol{W}_{\boldsymbol{x}}(\boldsymbol{t}-\boldsymbol{t}_0,\boldsymbol{f}-\boldsymbol{f}_0). \tag{7}$$

*Hermitian symmetry*. The WD of any signal $\boldsymbol{x}(\boldsymbol{t})$ features Hermitian symmetry,

$$\boldsymbol{W}_{\boldsymbol{x}}(\boldsymbol{t},\boldsymbol{f}) = \boldsymbol{W}_{\boldsymbol{x}}^{\mathrm{H}}(\boldsymbol{t},\boldsymbol{f}). \tag{8}$$

In particular, the diagonal elements of $\boldsymbol{W}_{\boldsymbol{x}}(\boldsymbol{t},\boldsymbol{f})$ are real-valued.

*Marginals and energy preservation*. In a certain sense, the WD can be interpreted as a TF energy distribution of $\boldsymbol{x}(\boldsymbol{t})$. This interpretation is supported by the marginal properties

$$\int_{\boldsymbol{t}} \boldsymbol{W}_{\boldsymbol{x}}(\boldsymbol{t},\boldsymbol{f})\,\mathrm{d}\boldsymbol{t} = \boldsymbol{X}(\boldsymbol{f})\boldsymbol{X}^{\mathrm{H}}(\boldsymbol{f}),$$

$$\int_{\boldsymbol{f}} \boldsymbol{W}_{\boldsymbol{x}}(\boldsymbol{t},\boldsymbol{f})\,\mathrm{d}\boldsymbol{f} = \boldsymbol{x}(\boldsymbol{t})\boldsymbol{x}^{\mathrm{H}}(\boldsymbol{t}),$$

where $\boldsymbol{X}(\boldsymbol{f}) \triangleq \int_{\boldsymbol{t}} \boldsymbol{x}(\boldsymbol{t})\mathrm{e}^{-\mathrm{j}2\pi\boldsymbol{f}^{\mathrm{T}}\boldsymbol{t}}\,\mathrm{d}\boldsymbol{t}$ denotes the $D$-dimensional Fourier transform of $\boldsymbol{x}(\boldsymbol{t})$. These marginal properties further imply the "energy preservation"

$$\int_{\boldsymbol{t}}\int_{\boldsymbol{f}} \boldsymbol{W}_{\boldsymbol{x}}(\boldsymbol{t},\boldsymbol{f})\,\mathrm{d}\boldsymbol{t}\,\mathrm{d}\boldsymbol{f} = \boldsymbol{E}_{\boldsymbol{x}} \triangleq \int_{\boldsymbol{t}} \boldsymbol{x}(\boldsymbol{t})\boldsymbol{x}^{\mathrm{H}}(\boldsymbol{t})\,\mathrm{d}\boldsymbol{t},$$

and further

$$\int_{\boldsymbol{t}}\int_{\boldsymbol{f}} \mathrm{Tr}\{\boldsymbol{W}_{\boldsymbol{x}}(\boldsymbol{t},\boldsymbol{f})\}\,\mathrm{d}\boldsymbol{t}\,\mathrm{d}\boldsymbol{f} = \|\boldsymbol{x}\|^2 \triangleq \int_{\boldsymbol{t}} \boldsymbol{x}^{\mathrm{H}}(\boldsymbol{t})\boldsymbol{x}(\boldsymbol{t})\,\mathrm{d}\boldsymbol{t}$$

(here, $\mathrm{Tr}\{\cdot\}$ denotes matrix trace).

*Moyal relation*. Let us define the inner product of $\boldsymbol{x}(\boldsymbol{t})$ and $\boldsymbol{y}(\boldsymbol{t})$ as

$$\langle \boldsymbol{x},\boldsymbol{y}\rangle \triangleq \int_{\boldsymbol{t}} \boldsymbol{y}^{\mathrm{H}}(\boldsymbol{t})\boldsymbol{x}(\boldsymbol{t})\,\mathrm{d}\boldsymbol{t}.$$

It is then possible to show the following extended Moyal relation:

$$\langle \boldsymbol{W}_{\boldsymbol{x}},\boldsymbol{W}_{\boldsymbol{y}}\rangle \triangleq \int_{\boldsymbol{t}}\int_{\boldsymbol{f}} \mathrm{Tr}\{\boldsymbol{W}_{\boldsymbol{x}}(\boldsymbol{t},\boldsymbol{f})\boldsymbol{W}_{\boldsymbol{y}}^{\mathrm{H}}(\boldsymbol{t},\boldsymbol{f})\}\,\mathrm{d}\boldsymbol{t}\,\mathrm{d}\boldsymbol{f} = |\langle \boldsymbol{x},\boldsymbol{y}\rangle|^2, \tag{9}$$

with the special case $\|\boldsymbol{W}_{\boldsymbol{x}}\|^2 = \|\boldsymbol{x}\|^4$. Note that (9) together with (7) and (8) implies that

$$\int_{\boldsymbol{t}'}\int_{\boldsymbol{f}'} \mathrm{Tr}\{\boldsymbol{W}_{\boldsymbol{x}}(\boldsymbol{t}',\boldsymbol{f}')\boldsymbol{W}_{\boldsymbol{w}}^{\mathrm{H}}(\boldsymbol{t}'-\boldsymbol{t},\boldsymbol{f}'-\boldsymbol{f})\}\,\mathrm{d}\boldsymbol{t}'\,\mathrm{d}\boldsymbol{f}' = |\langle \boldsymbol{x},\boldsymbol{w}_{\boldsymbol{t},\boldsymbol{f}}\rangle|^2,$$

where $\boldsymbol{w}_{\boldsymbol{t},\boldsymbol{f}}(\boldsymbol{t}') = (\mathbf{S}_{\boldsymbol{t},\boldsymbol{f}}\boldsymbol{w})(\boldsymbol{t}')$. This means that a local average of the WD (i.e., a smoothed version of the WD) can be interpreted as local energy of $\boldsymbol{x}(\boldsymbol{t})$ about the TF analysis point $(\boldsymbol{t},\boldsymbol{f})$.

*Finite support*. The time and frequency supports of the WD are given by the total time support of the signal and the total frequency support of its Fourier

transform, respectively:

$$\boldsymbol{x}(t)=\boldsymbol{0},\quad t\notin[t_1,t_2]$$
$$\Leftrightarrow\quad \boldsymbol{W}_x(t,f)=\boldsymbol{0},\quad t\notin[t_1,t_2],$$
$$\boldsymbol{X}(f)=\boldsymbol{0},\quad f\notin[f_1,f_2]$$
$$\Leftrightarrow\quad \boldsymbol{W}_x(t,f)=\boldsymbol{0},\quad f\notin[f_1,f_2].$$

*Symplectic covariance*. A property very specific of the WD is its covariance to area-preserving linear coordinate transforms. Such coordinate transforms are characterized by $2D\times 2D$ matrices $\boldsymbol{A}$ belonging to the symplectic group of dimension $2D$ [19]. The *metaplectic representation* [19] associates to each such matrix $\boldsymbol{A}$ a unitary operator $\boldsymbol{\mu}(\boldsymbol{A})$. The symplectic covariance of the WD is characterized by the relation

$$\boldsymbol{W}_{\boldsymbol{\mu}(\boldsymbol{A})\boldsymbol{x}}(t,f)=\boldsymbol{W}_{\boldsymbol{x}}\left(\boldsymbol{A}\begin{pmatrix}t\\ f\end{pmatrix}\right).$$

Special cases of the symplectic covariance property are as follows:

*TF scaling*:

$$\boldsymbol{A}=\begin{pmatrix}\boldsymbol{D}^{-1} & \boldsymbol{0}\\ \boldsymbol{0} & \boldsymbol{D}\end{pmatrix}$$
$$\Leftrightarrow(\boldsymbol{\mu}(\boldsymbol{A})\boldsymbol{x})(t)=\frac{1}{\sqrt{|\det\boldsymbol{D}|}}\,\boldsymbol{x}(\boldsymbol{D}^{-1}t)$$
$$\Leftrightarrow\boldsymbol{W}_{\boldsymbol{\mu}(\boldsymbol{A})\boldsymbol{x}}(t,f)=\boldsymbol{W}_{\boldsymbol{x}}(\boldsymbol{D}^{-1}t,\boldsymbol{D}f)$$

*Fourier transform*:

$$\boldsymbol{A}=\begin{pmatrix}\boldsymbol{0} & -\boldsymbol{I}T^2\\ \boldsymbol{I}/T^2 & \boldsymbol{0}\end{pmatrix}$$
$$\Leftrightarrow(\boldsymbol{\mu}(\boldsymbol{A})\boldsymbol{x})(t)=\frac{1}{T}\,\boldsymbol{X}\left(\frac{t}{T^2}\right)$$
$$\Leftrightarrow\boldsymbol{W}_{\boldsymbol{\mu}(\boldsymbol{A})\boldsymbol{x}}(t,f)=\boldsymbol{W}_{\boldsymbol{x}}\left(-T^2f,\frac{t}{T^2}\right)$$

*Chirp multiplication*:

$$\boldsymbol{A}=\begin{pmatrix}\boldsymbol{I} & \boldsymbol{0}\\ \boldsymbol{C} & \boldsymbol{I}\end{pmatrix}$$
$$\Leftrightarrow(\boldsymbol{\mu}(\boldsymbol{A})\boldsymbol{x})(t)=\mathrm{e}^{-\mathrm{j}\pi t^{\mathrm{T}}\boldsymbol{C}t}\boldsymbol{x}(t)$$
$$\Leftrightarrow\boldsymbol{W}_{\boldsymbol{\mu}(\boldsymbol{A})\boldsymbol{x}}(t,f)=\boldsymbol{W}_{\boldsymbol{x}}(t,f+\boldsymbol{C}t)$$

*Chirp convolution*:

$$\boldsymbol{A}=\begin{pmatrix}\boldsymbol{I} & \boldsymbol{B}\\ \boldsymbol{0} & \boldsymbol{I}\end{pmatrix}$$
$$\Leftrightarrow(\boldsymbol{\mu}(\boldsymbol{A})\boldsymbol{x})(t)=\frac{\mathrm{e}^{-\mathrm{j}\pi t^{\mathrm{T}}\boldsymbol{B}^{-1}t}}{\sqrt{|\det\boldsymbol{B}|}}*\boldsymbol{x}(t)$$
$$\Leftrightarrow\boldsymbol{W}_{\boldsymbol{\mu}(\boldsymbol{A})\boldsymbol{x}}(t,f)=\boldsymbol{W}_{\boldsymbol{x}}(t+\boldsymbol{B}f,f)$$

### 2.2. Weyl symbol

We next define an extended WS that is related to the WD of multidimensional vector signals. Consider a linear operator (LTV system) $\mathbf{H}$ that maps a multidimensional vector signal $\boldsymbol{x}(t)$ to another multidimensional vector signal $\boldsymbol{y}(t)$ of the same vector length[5] $K$ and the same signal dimension:

$$\boldsymbol{y}(t)=(\mathbf{H}\boldsymbol{x})(t)=\int_{t'}\boldsymbol{H}(t;t')\boldsymbol{x}(t')\,\mathrm{d}t',$$

with the $K\times K$ matrix kernel $\boldsymbol{H}(t;t')=[h_{k,l}(t;t')]$. We define the WS of such an operator $\mathbf{H}$ as the $K\times K$ matrix function

$$\boldsymbol{L}_{\mathbf{H}}(t,f)\triangleq\int_{\tau}\boldsymbol{H}\left(t+\frac{\tau}{2},t-\frac{\tau}{2}\right)\mathrm{e}^{-\mathrm{j}2\pi f^{\mathrm{T}}\tau}\,\mathrm{d}\tau.\qquad(10)$$

The WD in (6) is equal to the WS of the rank-one operator $\boldsymbol{x}\otimes\boldsymbol{x}^{\mathrm{H}}$ whose kernel equals $\boldsymbol{x}(t)\boldsymbol{x}^{\mathrm{H}}(t')$:

$$\mathbf{H}=\boldsymbol{x}\otimes\boldsymbol{x}^{\mathrm{H}}\quad\Leftrightarrow\quad\boldsymbol{L}_{\mathbf{H}}(t,f)=\boldsymbol{W}_{\boldsymbol{x}}(t,f).$$

Another link between WD and WS is provided by the relation

$$\langle\boldsymbol{L}_{\mathbf{H}},\boldsymbol{W}_{\boldsymbol{x}}\rangle=\langle\mathbf{H}\boldsymbol{x},\boldsymbol{x}\rangle,$$

which shows how quadratic forms can be reformulated in the TF domain.

In the following, we discuss important mathematical properties of the WS $\boldsymbol{L}_{\mathbf{H}}(t,f)$. These properties extend the properties summarized in Table 2.

*TF shift covariance*. For a TF shifted system $\tilde{\mathbf{H}}=\mathbf{S}_{t_0,f_0}\mathbf{H}\mathbf{S}_{t_0,f_0}^{+}$,

$$\boldsymbol{L}_{\tilde{\mathbf{H}}}(t,f)=\boldsymbol{L}_{\mathbf{H}}(t-t_0,f-f_0).$$

[5] The extension to the case of different vector lengths is straightforward.

*Adjoint*; *Hermitian symmetry*. The WS of the adjoint operator $\mathbf{H}^+$ is obtained by Hermitian transposition of $\boldsymbol{L}_{\mathbf{H}}(\boldsymbol{t},\boldsymbol{f})$,

$$\boldsymbol{L}_{\mathbf{H}^+}(\boldsymbol{t},\boldsymbol{f}) = \boldsymbol{L}_{\mathbf{H}}^{\mathrm{H}}(\boldsymbol{t},\boldsymbol{f}).$$

This implies that the WS of a self-adjoint operator $\mathbf{H} = \mathbf{H}^+$ features Hermitian symmetry,

$$\mathbf{H} = \mathbf{H}^+ \quad \Rightarrow \quad \boldsymbol{L}_{\mathbf{H}}(\boldsymbol{t},\boldsymbol{f}) = \boldsymbol{L}_{\mathbf{H}}^{\mathrm{H}}(\boldsymbol{t},\boldsymbol{f}).$$

In particular, in this case the diagonal elements of $\boldsymbol{L}_{\mathbf{H}}(\boldsymbol{t},\boldsymbol{f})$ are real-valued.

*Marginals and trace*. Under certain conditions, the WS $\boldsymbol{L}_{\mathbf{H}}(\boldsymbol{t},\boldsymbol{f})$ can be interpreted as a TF transfer function of $\mathbf{H}$. This interpretation is supported by the marginal properties

$$\int_{\boldsymbol{t}} \boldsymbol{L}_{\mathbf{H}}(\boldsymbol{t},\boldsymbol{f})\,\mathrm{d}\boldsymbol{t} = \hat{\boldsymbol{H}}(\boldsymbol{f},\boldsymbol{f}),$$

$$\int_{\boldsymbol{f}} \boldsymbol{L}_{\mathbf{H}}(\boldsymbol{t},\boldsymbol{f})\,\mathrm{d}\boldsymbol{f} = \boldsymbol{H}(\boldsymbol{t},\boldsymbol{t}),$$

where $\hat{\boldsymbol{H}}(\boldsymbol{f},\boldsymbol{f}')$ denotes the 2-D Fourier transform of $\boldsymbol{H}(\boldsymbol{t},\boldsymbol{t})$. These marginal properties imply the "trace preservation"

$$\int_{\boldsymbol{t}}\int_{\boldsymbol{f}} \boldsymbol{L}_{\mathbf{H}}(\boldsymbol{t},\boldsymbol{f})\,\mathrm{d}\boldsymbol{t}\,\mathrm{d}\boldsymbol{f} = \mathrm{tr}\{\mathbf{H}\},$$

where $\mathrm{tr}\{\mathbf{H}\} \triangleq \int_{\boldsymbol{t}} \boldsymbol{H}(\boldsymbol{t},\boldsymbol{t})\,\mathrm{d}\boldsymbol{t}$ denotes a matrix-valued operator trace (note the difference to the matrix trace denoted by $\mathrm{Tr}\{\cdot\}$).

*Moyal-type relation and energy*. A Moyal-type (i.e., inner product preservation) property of the WS is given by

$$\langle \boldsymbol{L}_{\mathbf{H}_1}, \boldsymbol{L}_{\mathbf{H}_2}\rangle = \langle \mathbf{H}_1, \mathbf{H}_2\rangle,$$

with the WS inner product defined as in (9) and the Hilbert–Schmidt operator inner product $\langle \mathbf{H}_1, \mathbf{H}_2\rangle = \int_{\boldsymbol{t}}\int_{\boldsymbol{t}'} \mathrm{Tr}\{\boldsymbol{H}_1(\boldsymbol{t},\boldsymbol{t}')\boldsymbol{H}_2^{\mathrm{H}}(\boldsymbol{t},\boldsymbol{t}')\}\,\mathrm{d}\boldsymbol{t}\,\mathrm{d}\boldsymbol{t}'$. In the case $\mathbf{H}_1 = \mathbf{H}_2 = \mathbf{H}$, this specializes to the norm preservation property

$$\|\boldsymbol{L}_{\mathbf{H}}\|^2 = \|\mathbf{H}\|^2,$$

with $\|\mathbf{H}\|^2 = \int_{\boldsymbol{t}}\int_{\boldsymbol{t}'} \mathrm{Tr}\{\boldsymbol{H}(\boldsymbol{t},\boldsymbol{t}')\boldsymbol{H}^{\mathrm{H}}(\boldsymbol{t},\boldsymbol{t}')\}\,\mathrm{d}\boldsymbol{t}\,\mathrm{d}\boldsymbol{t}'$ denoting the squared Hilbert–Schmidt operator norm.

*Finite support*. Let $\boldsymbol{H}^{(\mathrm{s})}(\boldsymbol{t},\boldsymbol{\tau}) \triangleq \boldsymbol{H}(\boldsymbol{t}+\frac{\boldsymbol{\tau}}{2},\boldsymbol{t}-\frac{\boldsymbol{\tau}}{2})$ and let $\hat{\boldsymbol{H}}^{(\mathrm{s})}(\boldsymbol{f},\boldsymbol{\nu})$ denote the Fourier transform of $\boldsymbol{H}^{(\mathrm{s})}(\boldsymbol{t},\boldsymbol{\tau})$. Then

$$\boldsymbol{H}^{(\mathrm{s})}(\boldsymbol{t},\boldsymbol{\tau}) = \mathbf{0}, \quad \boldsymbol{t} \notin [\boldsymbol{t}_1,\boldsymbol{t}_2]$$
$$\Leftrightarrow \quad \boldsymbol{L}_{\mathbf{H}}(\boldsymbol{t},\boldsymbol{f}) = \mathbf{0}, \quad \boldsymbol{t} \notin [\boldsymbol{t}_1,\boldsymbol{t}_2],$$
$$\hat{\boldsymbol{H}}^{(\mathrm{s})}(\boldsymbol{f},\boldsymbol{\nu}) = \mathbf{0}, \quad \boldsymbol{f} \notin [\boldsymbol{f}_1,\boldsymbol{f}_2]$$
$$\Leftrightarrow \quad \boldsymbol{L}_{\mathbf{H}}(\boldsymbol{t},\boldsymbol{f}) = \mathbf{0}, \quad \boldsymbol{f} \notin [\boldsymbol{f}_1,\boldsymbol{f}_2].$$

*Symplectic covariance*. Similarly to the WD, the WS is covariant to area-preserving linear coordinate transforms:

$$\boldsymbol{L}_{\boldsymbol{\mu}(\boldsymbol{A})\mathbf{H}\boldsymbol{\mu}(\boldsymbol{A})^+}(\boldsymbol{t},\boldsymbol{f}) = \boldsymbol{L}_{\mathbf{H}}\left(\boldsymbol{A}\begin{pmatrix}\boldsymbol{t}\\ \boldsymbol{f}\end{pmatrix}\right).$$

Special cases of the symplectic covariance property (TF scaling, Fourier transform, chirp multiplication, and chirp convolution) have been considered for the WD in Section 2.1.

## 3. Nonstationary random processes

We next consider a (generally nonstationary) random process $x(t)$ with zero mean and correlation function $r_x(t,t') = \mathrm{E}\{x(t)x^*(t')\}$. (We restrict our discussion to the scalar 1-D case although generalizations to multidimensional vector processes along the lines of Section 2 are straightforward.) Of course, the WD can be applied to an arbitrary realization of this process, so that the WD $W_x(t,f)$ is itself a 2-D random process. An immediate question of interest pertains to the *average* behavior of the WD. This is characterized by the expectation of $W_x(t,f)$—if it exists,

$$\overline{W}_x(t,f) \triangleq \mathrm{E}\{W_x(t,f)\} = \mathrm{E}\left\{\int_\tau x\left(t+\frac{\tau}{2}\right)x^*\left(t-\frac{\tau}{2}\right)\mathrm{e}^{-\mathrm{j}2\pi f\tau}\,\mathrm{d}\tau\right\}, \tag{11}$$

which is known as *Wigner–Ville spectrum* (WVS) [17,18,48,43]. (We note, however, that usually the definition of the WVS is based on Eq. (13) below.) The WVS can be loosely interpreted as a TF distribution

Table 3
Some properties of the WVS

| | |
|---|---|
| TF shift covariance | $\tilde{x}(t) = (\mathbf{S}_{t_0,f_0}x)(t) \Rightarrow \overline{W}_{\tilde{x}}(t,f) = \overline{W}_x(t-t_0, f-f_0)$ |
| Realvaluedness | $\overline{W}_x(t,f) = \overline{W}_x^*(t,f)$ |
| Marginal properties | $\int_t \overline{W}_x(t,f)\,\mathrm{d}t = r_X(f,f) = \mathrm{E}\{\lvert X(f)\rvert^2\}$ |
| | $\int_f \overline{W}_x(t,f)\,\mathrm{d}f = r_x(t,t) = \mathrm{E}\{\lvert x(t)\rvert^2\}$ |
| Mean energy | $\int_t \int_f \overline{W}_x(t,f)\,\mathrm{d}t\,\mathrm{d}f = \mathrm{E}\{\lVert x\rVert^2\},$ |
| Moyal-type relation | $\int_t \int_f \overline{W}_x(t,f)\overline{W}_y(t,f)\,\mathrm{d}t\,\mathrm{d}f = \langle \mathbf{R}_x, \mathbf{R}_y\rangle$ |
| Finite support | $r_x(t,t) = 0,\ t \notin [t_1,t_2] \Rightarrow \overline{W}_x(t,f) = 0,\ t \notin [t_1,t_2]$ |
| | $r_X(f,f) = 0,\ f \notin [f_1,f_2] \Rightarrow \overline{W}_x(t,f) = 0,\ f \notin [f_1,f_2]$ |
| Symplectic covariance | $\tilde{x}(t) = (\mu(\boldsymbol{A})x)(t) \Rightarrow \overline{W}_{\tilde{x}}(t,f) = \overline{W}_x(\boldsymbol{A}\binom{t}{f})$ |

of the mean energy of $x(t)$. In particular,

$$\overline{W}_x(t,f) *_t *_f W_w(-t,-f) = \mathrm{E}\{\lvert\langle x, w_{t,f}\rangle\rvert^2\} \geqslant 0. \tag{12}$$

Since $\mathrm{E}\{\lvert\langle x, w_{t,f}\rangle\rvert^2\}$ measures the average energy of $x(t)$ in a local neighborhood of the TF analysis point $(t,f)$, (12) shows that local averages of the WVS are measures of the mean local energy of $x(t)$ about $(t,f)$.

Under mild conditions [18], expectation and integration in (11) can be interchanged and we obtain

$$\begin{aligned}\overline{W}_x(t,f) &= \int_\tau r_x\left(t+\frac{\tau}{2}, t-\frac{\tau}{2}\right) \mathrm{e}^{-\mathrm{j}2\pi f\tau}\,\mathrm{d}\tau \\ &= L_{\mathbf{R}_x}(t,f),\end{aligned} \tag{13}$$

where $\mathbf{R}_x = \mathrm{E}\{x \otimes x^*\}$ denotes the correlation operator[6] of $x(t)$ and the last expression in (13) is obtained upon comparison with (3). We conclude that the WVS of $x(t)$ equals the WS of $\mathbf{R}_x$. An expression relating the WVS and the WD can be obtained by using the Karhunen–Loève (KL) eigenexpansion [17], $\mathbf{R}_x = \sum_k \lambda_k u_k \otimes u_k^*$. Here, $\lambda_k \geqslant 0$ are the KL eigenvalues and $\{u_k(t)\}$ is the orthonormal basis of KL eigenfunctions. Inserting this expansion into (13), we obtain

$$\overline{W}_x(t,f) = \sum_k \lambda_k W_{u_k}(t,f).$$

Thus, the WVS is a weighted sum of the WDs of the KL eigenfunctions with the KL eigenvalues being the corresponding weights.

The invertibility of the WS (cf. (4)) implies that the correlation function $r_x(t,t')$ can be reobtained from the WVS, and thus, the WVS constitutes a complete second-order statistics of $x(t)$. Further mathematical properties of the WVS that justify an interpretation as mean TF energy spectrum (or time-varying power spectrum) are listed in Table 3.

A feature distinguishing the WVS (i.e., the expected WD) from the WD pertains to the occurrence of cross terms. While in the WD oscillating and partly negative cross terms will *always* occur midway between any two signal components [25], the presence of cross terms in the WVS is determined by the TF correlations of the process [44,48] (the WVS cross terms are therefore sometimes termed *statistical cross terms*). Random processes featuring correlations only between closely spaced TF points are called *underspread* [39,41,44,48]. Their WVS features virtually no statistical cross terms. On the other hand, the WVS of *overspread* processes (i.e., processes for which even widely spaced TF points

[6] The correlation operator of a random process $x(t)$ is the positive (semi-)definite linear operator with kernel $r_x(t,t')$.

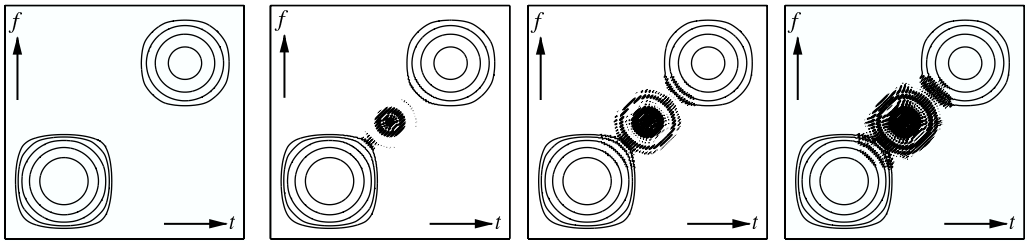


Fig. 3. WVS of four random processes with increasing levels of TF correlation.

are strongly correlated) contains significant statistical cross terms. The relation of statistical cross terms to TF correlations is corroborated by the following result that applies to Gaussian random processes. Let

$$\begin{aligned}&\mathscr{C}_x(t,f;\tau,\nu)\\&\triangleq \operatorname{cov}\left\{W_x\left(t+\frac{\tau}{2},f+\frac{\nu}{2}\right),W_x\left(t-\frac{\tau}{2},f-\frac{\nu}{2}\right)\right\}\\&=\mathrm{E}\left\{\left[W_x\left(t+\frac{\tau}{2},f+\frac{\nu}{2}\right)-\overline{W}_x\left(t+\frac{\tau}{2},f+\frac{\nu}{2}\right)\right]\right.\\&\quad\left.\times\left[W_x\left(t-\frac{\tau}{2},f-\frac{\nu}{2}\right)-\overline{W}_x\left(t-\frac{\tau}{2},f-\frac{\nu}{2}\right)\right]\right\}.\end{aligned}$$

Remarkably, this WD covariance can be shown to equal the (coordinate-transformed) *transfer Wigner distribution* of the correlation operator $\mathbf{R}_x$ (cf. (16) in Section 4),

$$\mathscr{C}_x(t,f;\tau,\nu)=\widetilde{W}_{\mathbf{R}_x}(t,f;\tau,\nu).$$

For fixed $(t,f)$, $\mathscr{C}_x(t,f;\tau,\nu)$ characterizes the correlation of all WD values that lie symmetrically about $(t,f)$ and are separated by $\tau$ in time and by $\nu$ in frequency. The overall correlation of WD components about $(t,f)$ is obtained by integrating over $\tau$ and $\nu$, which can be shown to yield the squared WVS at $(t,f)$:

$$\int_\tau\int_\nu \mathscr{C}_x(t,f;\tau,\nu)\,\mathrm{d}\tau\,\mathrm{d}\nu=\overline{W}_x^2(t,f).$$

This demonstrates that large values of $\overline{W}_x(t,f)$ are not necessarily due to energetic contributions of $x(t)$ about $(t,f)$ but may also be the result of strong TF correlations of process components lying symmetrically with respect to $(t,f)$.

The application of the WVS to statistical signal processing (nonstationary signal estimation and detection) is discussed in [16,28,30,31,46,49,62].

**Example 1.** As an illustration of the WVS and statistical cross terms, we consider a synthetic random process that consists of two effectively TF disjoint, underspread "subprocesses", i.e., $x(t)=x_1(t)+x_2(t)$. If $x_1(t)$ and $x_2(t)$ are uncorrelated, $x(t)$ is underspread and there simply is $\overline{W}_x(t,f)=\overline{W}_{x_1}(t,f)+\overline{W}_{x_2}(t,f)$. Here, the WVS of $x(t)$ does not contain statistical cross terms and correctly indicates the mean energy distribution of $x(t)$, as depicted in Fig. 3(a). However, for increasing correlation between $x_1(t)$ and $x_2(t)$, $x(t)$ becomes more and more overspread. This is reflected by the statistical cross terms—indicating the TF correlation between $x_1(t)$ and $x_2(t)$—that become more and more pronounced as shown in Fig. 3(b)–(d). Since these statistical cross terms are partly negative, they prevent an interpretation of $\overline{W}_x(t,f)$ as mean TF energy distribution. Note, however, that according to (12) suitable local averages of the WVS correctly indicate that $x(t)$ features no energy at the TF locations of the statistical cross terms.

**Example 2.** Next, we consider the application of the WVS to the spectral analysis of pressure signals measured in a car engine during knocking combustions (cf. Section 1.1). This application was possible since an ensemble of observations (several recorded pressure signals) was available. Estimates of the WVS were obtained by replacing the expectation (i.e., the true ensemble average) with the average of the WDs of the individual observations. Fig. 4 shows the resulting WVS estimates obtained for engine speeds of 1000, 2000, and 4000 rpm. These spectrum estimates

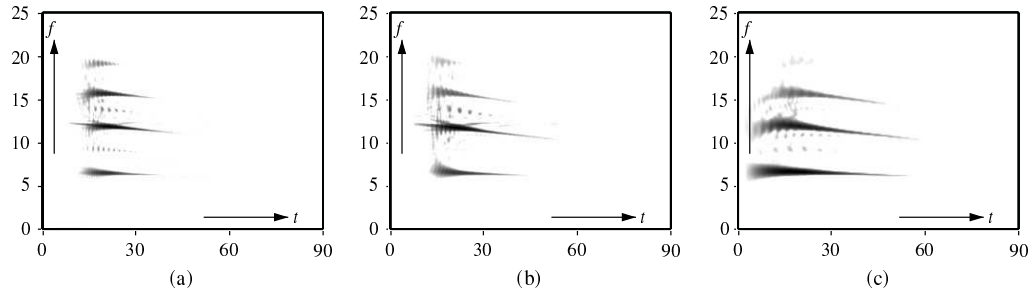


Fig. 4. Estimated WVS of pressure signals measured in a car engine running at (a) 1000 rpm, (b) 2000 rpm, and (c) 4000 rpm. Horizontal axis is crank angle (which is proportional to time), vertical axis is frequency in kHz. This figure should be compared to Fig. 1.

show that the pressure signals consist of several resonance components whose frequencies decrease with time. A comparison with Fig. 1 shows that the WVS features much less cross terms than the WD of a single realization. This is because the individual resonance components are effectively uncorrelated [37], i.e., the pressure signal process is reasonably underspread.

## 4. Linear time-varying systems

An interesting alternative to the WS for the TF description of an LTV system $\mathbf{H}$ is the *transfer Wigner distribution* (TWD), defined as [1,29,42]

$$\mathscr{W}_{\mathbf{H}}(t,f;t',f') \triangleq \int_{\tau}\int_{\tau'} h\left(t+\frac{\tau}{2},t'+\frac{\tau'}{2}\right) \times h^{*}\left(t-\frac{\tau}{2},t'-\frac{\tau'}{2}\right) \mathrm{e}^{-\mathrm{j}2\pi(f\tau-f'\tau')}\,\mathrm{d}\tau\,\mathrm{d}\tau'.$$

Comparing with (6), it is seen that the TWD (up to a minus sign in the exponent) is a special case of the WD of a scalar 2-D ($K=1, D=2$) "signal", the signal actually being the impulse response $h(t,t')$ of $\mathbf{H}$. Consequently, the TWD is a *quadratic* system representation (in contrast to the WS, which is a linear system representation). The TWD describes the mapping of the WD of the input signal $x(t)$ to the WD of the output signal $(\mathbf{H}x)(t)$ via the relation

$$W_{\mathbf{H}x}(t,f)=\int_{t'}\int_{f'} \mathscr{W}_{\mathbf{H}}(t,f;t',f')W_x(t',f')\,\mathrm{d}t'\,\mathrm{d}f'.$$

Hence, with certain precautions, $\mathscr{W}_{\mathbf{H}}(t,f;t',f')$ can be viewed as a measure of the amount of energy that the LTV system $\mathbf{H}$ transfers from the TF point $(t',f')$ to the TF point $(t,f)$. Further mathematical properties of the TWD are summarized in Table 4.

Integrating the TWD $\mathscr{W}_{\mathbf{H}}(t,f;t',f')$ with respect to $(t,f)$ and $(t',f')$ yields the so-called *input Wigner distribution* (IWD) and *output Wigner distribution* (OWD) of $\mathbf{H}$, respectively [29], i.e.,

$$W_{\mathbf{H}}^{(\mathrm{I})}(t,f) \triangleq \int_{t_1}\int_{f_1} \mathscr{W}_{\mathbf{H}}(t_1,f_1;t,f)\,\mathrm{d}t_1\,\mathrm{d}f_1,$$

$$W_{\mathbf{H}}^{(\mathrm{O})}(t,f) \triangleq \int_{t'}\int_{f'} \mathscr{W}_{\mathbf{H}}(t,f;t',f')\,\mathrm{d}t'\,\mathrm{d}f'.$$

The IWD describes how much energy is picked up by the system $\mathbf{H}$ at the TF point $(t,f)$. Thus, the effective support of the IWD characterizes the TF region where the system $\mathbf{H}$ can pick up energy. In contrast, the OWD describes how much energy is delivered (on average) by $\mathbf{H}$ at the TF point $(t,f)$, and thus its effective support equals the TF region where the output signals of $\mathbf{H}$ are potentially located. Using the singular value decomposition [55] $\mathbf{H}=\sum_k \sigma_k u_k \otimes v_k^*$ (where $\sigma_k$, $u_k(t)$, and $v_k(t)$ denote the singular values, left singular functions, and right singular functions, respectively), one can show

$$W_{\mathbf{H}}^{(\mathrm{I})}(t,f)=\sum_k \sigma_k^2 W_{v_k}(t,f),$$

$$W_{\mathbf{H}}^{(\mathrm{O})}(t,f)=\sum_k \sigma_k^2 W_{u_k}(t,f). \qquad (14)$$

Table 4
Some properties of the TWD

| | |
|---|---|
| Input TF shift | $\tilde{\mathbf{H}} = \mathbf{H}\mathbf{S}^{+}_{t_0,f_0} \Rightarrow \mathcal{W}_{\tilde{\mathbf{H}}}(t,f;t',f') = \mathcal{W}_{\mathbf{H}}(t,f;t'-t_0,f'-f_0)$ |
| Output TF shift | $\tilde{\mathbf{H}} = \mathbf{S}_{t_0,f_0}\mathbf{H} \Rightarrow \mathcal{W}_{\tilde{\mathbf{H}}}(t,f;t',f') = \mathcal{W}_{\mathbf{H}}(t-t_0,f-f_0;t',f')$ |
| Realvaluedness | $\mathcal{W}_{\mathbf{H}}(t,f;t',f') = \mathcal{W}^{*}_{\mathbf{H}}(t,f;t',f')$ |
| Marginal properties I | $\int_t \int_{t'} \mathcal{W}_{\mathbf{H}}(t,f;t',f')\,\mathrm{d}t\,\mathrm{d}t' = \lvert H(f,f')\rvert^2$ |
| | $\int_f \int_{f'} \mathcal{W}_{\mathbf{H}}(t,f;t',f')\,\mathrm{d}f\,\mathrm{d}f' = \lvert h(t,t')\rvert^2$ |
| Marginal properties II | $\int_{t'} \int_{f'} \mathcal{W}_{\mathbf{H}}(t,f;t',f')\,\mathrm{d}t'\,\mathrm{d}f' = W^{(\mathrm{O})}_{\mathbf{H}}(t,f)$ |
| | $\int_t \int_f \mathcal{W}_{\mathbf{H}}(t,f;t',f')\,\mathrm{d}t\,\mathrm{d}f = W^{(\mathrm{I})}_{\mathbf{H}}(t',f')$ |
| Energy | $\int_t \int_f \int_{t'} \int_{f'} \mathcal{W}_{\mathbf{H}}(t,f;t',f')\,\mathrm{d}t\,\mathrm{d}f\,\mathrm{d}t'\,\mathrm{d}f' = \lVert\mathbf{H}\rVert^2$ |
| | $\int_t \int_f \int_{t'} \int_{f'} \mathcal{W}^2_{\mathbf{H}}(t,f;t',f')\,\mathrm{d}t\,\mathrm{d}f\,\mathrm{d}t'\,\mathrm{d}f' = \lVert\mathbf{H}\rVert^4$ |
| Moyal-type relation | $\langle \mathcal{W}_{\mathbf{H}_1}, \mathcal{W}_{\mathbf{H}_2}\rangle = \lvert\langle \mathbf{H}_1, \mathbf{H}_2\rangle\rvert^2$ |
| Finite support | $h(t,t') = 0,\ t' \notin [t_1,t_2] \Rightarrow \mathcal{W}_{\mathbf{H}}(t,f;t',f') = 0,\ t' \notin [t_1,t_2]$ |
| | $h(t,t') = 0,\ t \notin [t_1,t_2] \Rightarrow \mathcal{W}_{\mathbf{H}}(t,f;t',f') = 0,\ t \notin [t_1,t_2]$ |
| | $H(f,f') = 0,\ f' \notin [f_1,f_2] \Rightarrow \mathcal{W}_{\mathbf{H}}(t,f;t',f') = 0,\ f' \notin [f_1,f_2]$ |
| | $H(f,f') = 0,\ f \notin [f_1,f_2] \Rightarrow \mathcal{W}_{\mathbf{H}}(t,f;t',f') = 0,\ f \notin [f_1,f_2]$ |
| Symplectic covariance | $\tilde{\mathbf{H}} = \mathbf{H}\mu(A)^{+} \Rightarrow \mathcal{W}_{\tilde{\mathbf{H}}}(t,f;t',f') = \mathcal{W}_{\mathbf{H}}(t,f;A\binom{t'}{f'})$ |
| | $\tilde{\mathbf{H}} = \mu(A)\mathbf{H} \Rightarrow \mathcal{W}_{\tilde{\mathbf{H}}}(t,f;t',f') = \mathcal{W}_{\mathbf{H}}(A\binom{t}{f};t',f')$ |

These relations provide a link between the IWD/OWD and the ordinary WD. Since the left and right singular functions span the signal spaces where $\mathbf{H}$ respectively delivers and picks up energy, (14) further supports the above-mentioned interpretations of the IWD and OWD.

The IWD and OWD can also be related to the WS via the expressions

$$W^{(\mathrm{I})}_{\mathbf{H}}(t,f) = L_{\mathbf{H}^{+}\mathbf{H}}(t,f),$$

$$W^{(\mathrm{O})}_{\mathbf{H}}(t,f) = L_{\mathbf{H}\mathbf{H}^{+}}(t,f). \tag{15}$$

Hence, it is seen that in the case of a normal system (i.e., a system satisfying $\mathbf{H}\mathbf{H}^{+} = \mathbf{H}^{+}\mathbf{H}$ [55]), the IWD and OWD coincide. Further mathematical properties of the IWD and OWD are summarized in Tables 5 and 6.

The OWD can be linked to the spectral analysis of nonstationary processes. For a nonstationary random process $x(t)$, consider the *innovations system representation* that is given by the input–output relation $x(t) = (\mathbf{H}_x n)(t) = \int_t h_x(t,t')n(t')\,\mathrm{d}t'$, where $n(t)$ denotes normalized stationary white noise and $h_x(t,t')$ is the kernel of an innovations system $\mathbf{H}_x$ of $x(t)$ [12,57]. The correlation operator of $x(t)$ can be written in terms of the innovations system $\mathbf{H}_x$ as $\mathbf{R}_x = \mathbf{H}_x\mathbf{H}_x^{+}$. Comparing (15) and (13), it is then seen that the WVS of $x(t)$ equals the OWD of the innovations system $\mathbf{H}_x$,

$$\overline{W}_x(t,f) = L_{\mathbf{R}_x}(t,f) = L_{\mathbf{H}_x\mathbf{H}_x^{+}}(t,f) = W^{(\mathrm{O})}_{\mathbf{H}_x}(t,f).$$

Table 5
Some properties of the IWD (**U** denotes a unitary operator)

| | |
|---|---|
| Input TF shift | $\tilde{\mathbf{H}} = \mathbf{H}\mathbf{S}^{+}_{t_0,f_0} \Rightarrow W^{(\mathrm{I})}_{\tilde{\mathbf{H}}}(t,f) = W^{(\mathrm{I})}_{\mathbf{H}}(t-t_0, f-f_0)$ |
| Output TF shift | $\tilde{\mathbf{H}} = \mathbf{S}_{t_0,f_0}\mathbf{H} \Rightarrow W^{(\mathrm{I})}_{\tilde{\mathbf{H}}}(t,f) = W^{(\mathrm{I})}_{\mathbf{H}}(t,f)$ |
| Realvaluedness | $W^{(\mathrm{I})}_{\mathbf{H}}(t,f) = W^{(\mathrm{I})*}_{\mathbf{H}}(t,f)$ |
| Marginal properties | $\int_t W^{(\mathrm{I})}_{\mathbf{H}}(t,f)\,\mathrm{d}t = (\mathbf{H}^{+}\mathbf{H})(f,f)$ |
| | $\int_f W^{(\mathrm{I})}_{\mathbf{H}}(t,f)\,\mathrm{d}f = (\mathbf{H}^{+}\mathbf{H})(t,t)$ |
| Energy | $\int_t\int_f W^{(\mathrm{I})}_{\mathbf{H}}(t,f)\,\mathrm{d}t\,\mathrm{d}f = \|\mathbf{H}\|^2$ |
| Moyal-type relation | $\int_t\int_f W^{(\mathrm{I})}_{\mathbf{H}_1}(t,f) W^{(\mathrm{I})}_{\mathbf{H}_2}(t,f)\,\mathrm{d}t\,\mathrm{d}f = \|\mathbf{H}_1\mathbf{H}_2^{+}\|^2$ |
| Finite support | $h(t,t') = 0,\ t' \notin [t_1,t_2] \Rightarrow W^{(\mathrm{I})}_{\mathbf{H}}(t,f) = 0,\ t \notin [t_1,t_2]$ |
| | $H(f,f') = 0,\ f' \notin [f_1,f_2] \Rightarrow W^{(\mathrm{I})}_{\mathbf{H}}(t,f) = 0,\ f \notin [f_1,f_2]$ |
| Symplectic covariance | $\tilde{\mathbf{H}} = \mathbf{H}\mu(\boldsymbol{A})^{+} \Rightarrow W^{(\mathrm{I})}_{\tilde{\mathbf{H}}}(t,f) = W^{(\mathrm{I})}_{\mathbf{H}}(\boldsymbol{A}\binom{t}{f})$ |
| Unitary invariance | $\tilde{\mathbf{H}} = \mathbf{U}\mathbf{H} \Rightarrow W^{(\mathrm{I})}_{\tilde{\mathbf{H}}}(t,f) = W^{(\mathrm{I})}_{\mathbf{H}}(t,f)$ |

Table 6
Some properties of the OWD

| | |
|---|---|
| Input TF shift | $\tilde{\mathbf{H}} = \mathbf{H}\mathbf{S}^{+}_{t_0,f_0} \Rightarrow W^{(\mathrm{O})}_{\tilde{\mathbf{H}}}(t,f) = W^{(\mathrm{O})}_{\mathbf{H}}(t,f)$ |
| Output TF shift | $\tilde{\mathbf{H}} = \mathbf{S}_{t_0,f_0}\mathbf{H} \Rightarrow W^{(\mathrm{O})}_{\tilde{\mathbf{H}}}(t,f) = W^{(\mathrm{O})}_{\mathbf{H}}(t-t_0, f-f_0)$ |
| Realvaluedness | $W^{(\mathrm{O})}_{\mathbf{H}}(t,f) = W^{(\mathrm{O})*}_{\mathbf{H}}(t,f)$ |
| Marginal properties | $\int_t W^{(\mathrm{O})}_{\mathbf{H}}(t,f)\,\mathrm{d}t = (\mathbf{H}\mathbf{H}^{+})(f,f)$ |
| | $\int_f W^{(\mathrm{O})}_{\mathbf{H}}(t,f)\,\mathrm{d}f = (\mathbf{H}\mathbf{H}^{+})(t,t)$ |
| Energy | $\int_t\int_f W^{(\mathrm{O})}_{\mathbf{H}}(t,f)\,\mathrm{d}t\,\mathrm{d}f = \|\mathbf{H}\|^2$ |
| Moyal-type relation | $\int_t\int_f W^{(\mathrm{O})}_{\mathbf{H}_1}(t,f) W^{(\mathrm{O})}_{\mathbf{H}_2}(t,f)\,\mathrm{d}t\,\mathrm{d}f = \|\mathbf{H}_1^{+}\mathbf{H}_2\|^2$ |
| Finite support | $h(t,t') = 0,\ t \notin [t_1,t_2] \Rightarrow W^{(\mathrm{O})}_{\mathbf{H}}(t,f) = 0,\ t \notin [t_1,t_2]$ |
| | $H(f,f') = 0,\ f \notin [f_1,f_2] \Rightarrow W^{(\mathrm{O})}_{\mathbf{H}}(t,f) = 0,\ f \notin [f_1,f_2]$ |
| Symplectic covariance | $\tilde{\mathbf{H}} = \mu(\boldsymbol{A})\mathbf{H} \Rightarrow W^{(\mathrm{O})}_{\tilde{\mathbf{H}}}(t,f) = W^{(\mathrm{O})}_{\mathbf{H}}(\boldsymbol{A}\binom{t}{f})$ |
| Unitary invariance | $\tilde{\mathbf{H}} = \mathbf{H}\mathbf{U} \Rightarrow W^{(\mathrm{O})}_{\tilde{\mathbf{H}}}(t,f) = W^{(\mathrm{O})}_{\mathbf{H}}(t,f)$ |

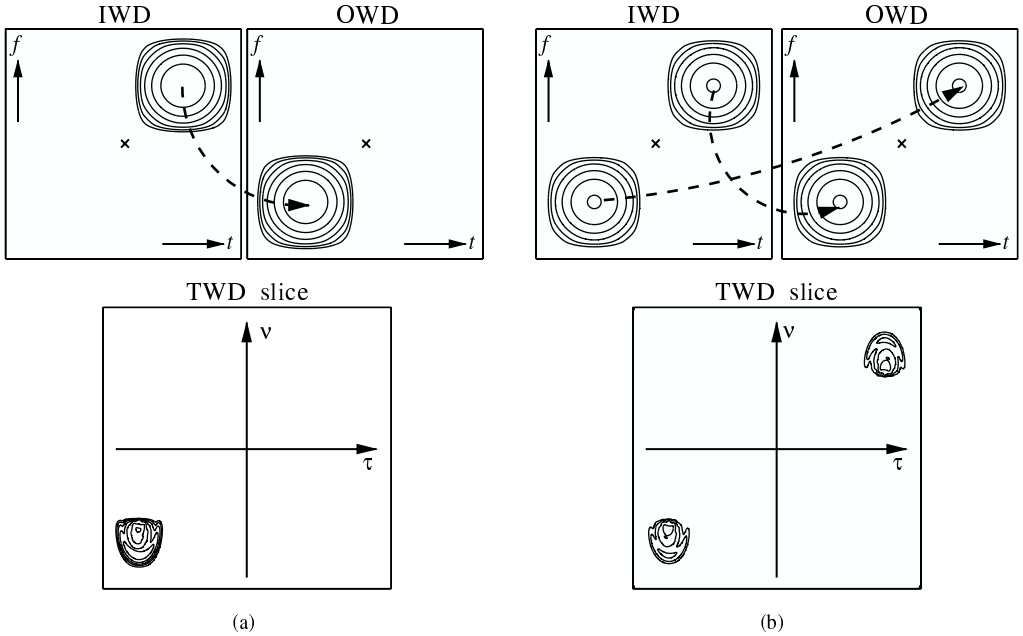


Fig. 5. IWD, OWD, and TWD slice of two overspread systems: (a) System causing a unidirectional energy transfer (indicated by dashed arrow) from upper right to lower left corner, (b) system causing a bidirectional energy transfer between upper right and lower left corner.

Let us finally consider the following coordinate-transformed version of the TWD,

$$\widetilde{W}_{\mathbf{H}}(t,f;\tau,\nu) \triangleq W_{\mathbf{H}}\left(t+\frac{\tau}{2},f+\frac{\nu}{2};t-\frac{\tau}{2},f-\frac{\nu}{2}\right). \tag{16}$$

Remarkably, this coordinate-transformed WD of the "signal" $h(t,t')$ can be shown to equal the WD of the "signal" $L_{\mathbf{H}}(t,f)$, i.e.,

$$\begin{aligned}\widetilde{W}_{\mathbf{H}}(t,f;\tau,\nu) &= \int_{\Delta t}\int_{\Delta f} L_{\mathbf{H}}\left(t+\frac{\Delta t}{2},f+\frac{\Delta f}{2}\right)\\ &\quad\times L_{\mathbf{H}}^{*}\left(t-\frac{\Delta t}{2},f-\frac{\Delta f}{2}\right)\\ &\quad\times \mathrm{e}^{-\mathrm{j}2\pi(\nu\Delta t-\tau\Delta f)}\,\mathrm{d}\Delta t\,\mathrm{d}\Delta f.\end{aligned} \tag{17}$$

From this expression, it follows that

$$\int_{\tau}\int_{\nu}\widetilde{W}_{\mathbf{H}}(t,f;\tau,\nu)\,\mathrm{d}\tau\,\mathrm{d}\nu = |L_{\mathbf{H}}(t,f)|^2.$$

An interpretation of this relation was provided in Section 1.2 (cf. the discussion around (5)).

**Example.** The IWD, OWD, and TWD of two synthetic LTV systems are shown in Fig. 5. Both LTV systems are *overspread*, i.e., they introduce significant TF shifts. Indeed, in the case of the first system (Fig. 5(a)), these TF shifts are obvious from the fact that the TF supports of the IWD and OWD (i.e., the TF regions where energy is picked up and delivered, respectively) are effectively disjoint. This energy transfer "to the left and down" is also correctly indicated by the TWD slice $\widetilde{W}_{\mathbf{H}}(t_0,f_0;\tau,\nu)$ with the TF center point $(t_0,f_0)$ chosen as indicated by the cross in the IWD and OWD plots.

In contrast, for the second system (Fig. 5(b)), the IWD and OWD are seen to be completely equal, i.e., the TF regions where energy is picked up and where energy is delivered are the same. Nonetheless, the system introduces significant TF shifts. Indeed, the TWD slice $\widetilde{W}_{\mathbf{H}}(t_0,f_0;\tau,\nu)$ (with $(t_0,f_0)$ chosen as in part (a)) shows that the energy picked up in the upper right corner is completely transferred to the lower left

corner and vice versa. We note that for these examples none of the conclusions drawn from the IWD, OWD, and TWD could have been obtained from the WS in a similarly simple and clear manner.

## 5. Random time-varying systems

In certain cases, the LTV system $\mathbf{H}$ under consideration is modeled as being random, i.e., impulse response $h(t,t')$ and WS $L_{\mathbf{H}}(t,f)$ are 2-D random processes. A particularly important application is the modeling of wireless communication channels that are generally characterized by random multipath propagation and Doppler shifts [60]. Usually, in this context the assumption of *wide-sense stationary uncorrelated scattering* (WSSUS) is made [2,52], which amounts to assuming that $L_{\mathbf{H}}(t,f)$ is a 2-D stationary process. This means that the 4-D correlation function of $L_{\mathbf{H}}(t,f)$,

$$r_{\mathbf{H}}(t,f;\Delta t,\Delta f) \triangleq \mathrm{E}\left\{L_{\mathbf{H}}\left(t+\frac{\Delta t}{2},f+\frac{\Delta f}{2}\right) \times L_{\mathbf{H}}^{*}\left(t-\frac{\Delta t}{2},f-\frac{\Delta f}{2}\right)\right\}, \tag{18}$$

is independent of $t$ and $f$. Thus, $r_{\mathbf{H}}(t,f;\Delta t,\Delta f) = \tilde{r}_{\mathbf{H}}(\Delta t,\Delta f)$ where $\tilde{r}_{\mathbf{H}}(\Delta t,\Delta f)$ is termed the *TF correlation function* [2,52]. The WSSUS assumption allows the use of "stationary" techniques for the characterization of random LTV channels. In particular, the *scattering function* [2,52]

$$C_{\mathbf{H}}(\tau,\nu) \triangleq \int_{\Delta t}\int_{\Delta f} \tilde{r}_{\mathbf{H}}(\Delta t,\Delta f) \times \mathrm{e}^{-\mathrm{j}2\pi(\nu\Delta t-\tau\Delta f)}\,\mathrm{d}\Delta t\,\mathrm{d}\Delta f \tag{19}$$

is the power spectral density of $L_{\mathbf{H}}(t,f)$. It describes the mean power of scatterers causing a time delay $\tau$ and a Doppler frequency shift $\nu$. Just as $\tilde{r}_{\mathbf{H}}(\Delta t,\Delta f)$, the scattering function is a complete description of the second-order statistics of a WSSUS channel.

In practice, the WSSUS assumption holds only approximately within certain time and frequency intervals. In this case, the scattering function is no longer defined. It is thus of interest to find an extension of the scattering function that applies to non-WSSUS channels, i.e., channels whose WS is a 2-D *non*stationary process. By analogy to (19) and (13), we introduce the *local scattering function* [45]

$$\mathscr{C}_{\mathbf{H}}(t,f;\tau,\nu) \triangleq \int_{\Delta t}\int_{\Delta f} r_{\mathbf{H}}(t,f;\Delta t,\Delta f) \times \mathrm{e}^{-\mathrm{j}2\pi(\nu\Delta t-\tau\Delta f)}\,\mathrm{d}\Delta t\,\mathrm{d}\Delta f. \tag{20}$$

It can be shown [45] that $\mathscr{C}_{\mathbf{H}}(t,f;\tau,\nu)$ characterizes the mean power of scatterers causing a delay $\tau$ and Doppler shift $\nu$ of input signal components localized about $(t,f)$. In the case of a WSSUS system, $\mathscr{C}_{\mathbf{H}}(t,f;\tau,\nu) = C_{\mathbf{H}}(\tau,\nu)$. Some properties of $\mathscr{C}_{\mathbf{H}}(t,f;\tau,\nu)$ are listed in Table 7.

We finally discuss some relations of the local scattering function $\mathscr{C}_{\mathbf{H}}(t,f;\tau,\nu)$ with various other TF representations considered previously. First, by comparing (20) and (18) with (17), it is seen that

$$\mathscr{C}_{\mathbf{H}}(t,f;\tau,\nu) = \mathrm{E}\{\widetilde{\mathscr{W}}_{\mathbf{H}}(t,f;\tau,\nu)\},$$

provided that the integration and expectation in (20) can be interchanged. Since $\widetilde{\mathscr{W}}_{\mathbf{H}}(t,f;\tau,\nu)$ can be interpreted as the WD of $L_{\mathbf{H}}(t,f)$, it follows that $\mathscr{C}_{\mathbf{H}}(t,f;\tau,\nu)$ can be viewed as the WVS (cf. (11)) of the 2-D process $L_{\mathbf{H}}(t,f)$, i.e., $\mathscr{C}_{\mathbf{H}}(t,f;\tau,\nu) = \overline{W}_{L_{\mathbf{H}}}(t,f;\tau,\nu)$. This suggests that the local scattering function can be written in terms of the WS. In fact, comparing (20) and (10) (with $K=1$, $D=2$) shows that

$$\mathscr{C}_{\mathbf{H}}(t,f;\tau,\nu) = \overline{W}_{L_{\mathbf{H}}}(t,f;\tau,\nu) = L_{\mathbf{R}_{\mathbf{H}}}(t,f;\tau,\nu),$$

where $\mathbf{R}_{\mathbf{H}}$ denotes the correlation operator whose 4-D kernel is the correlation function $\mathrm{E}\{L_{\mathbf{H}}(t,f)L_{\mathbf{H}}^{*}(t',f')\}$ of $L_{\mathbf{H}}(t,f)$.

**Example.** We illustrate the application of the local scattering function $\mathscr{C}_{\mathbf{H}}(t,f;\tau,\nu)$ to a measured[7] non-WSSUS channel (suburban, partial line-of-sight scenario). During the measurement duration of 50 s, the mobile moved around a corner with a constant velocity of 1.6 m/s and approached the base station.

[7] The measurements were performed in the course of the METAMORP project [34]. We are grateful to T-NOVA Deutsche Telekom Innovationsgesellschaft mbH (Technologiezentrum Darmstadt, Germany) and to I. Gaspard and M. Steinbauer for providing us with the measurement data.

Table 7
Some properties of the local scattering function

| | |
|---|---|
| TF shift covariance | $\tilde{\mathbf{H}} = \mathbf{S}_{t_0,f_0}\mathbf{H}\mathbf{S}_{t_0,f_0}^{+} \Rightarrow \mathscr{C}_{\tilde{\mathbf{H}}}(t,f;\tau,\nu) = \mathscr{C}_{\mathbf{H}}(t-t_0, f-f_0;\tau,\nu)$ |
| Realvaluedness | $\mathscr{C}_{\mathbf{H}}(t,f;\tau,\nu) = \mathscr{C}_{\mathbf{H}}^{*}(t,f;\tau,\nu)$ |
| Marginal properties | $\int_t\int_\tau \mathscr{C}_{\mathbf{H}}(t,f;\tau,\nu)\,\mathrm{d}t\,\mathrm{d}\tau = \mathrm{E}\{\lvert H^{(\mathrm{s})}(f,\nu)\rvert^2\}$ |
| | $\int_f\int_\nu \mathscr{C}_{\mathbf{H}}(t,f;\tau,\nu)\,\mathrm{d}f\,\mathrm{d}\nu = \mathrm{E}\{\lvert h^{(\mathrm{s})}(t,\tau)\rvert^2\}$ |
| | $\int_\tau\int_\nu \mathscr{C}_{\mathbf{H}}(t,f;\tau,\nu)\,\mathrm{d}\tau\,\mathrm{d}\nu = \mathrm{E}\{\lvert L_{\mathbf{H}}(t,f)\rvert^2\}$ |
| Mean energy | $\int_t\int_f\int_\tau\int_\nu \mathscr{C}_{\mathbf{H}}(t,f;\tau,\nu)\,\mathrm{d}t\,\mathrm{d}f\,\mathrm{d}\tau\,\mathrm{d}\nu = \mathrm{E}\{\lVert\mathbf{H}\rVert^2\}$ |
| Finite support | $h^{(\mathrm{s})}(t,\tau)=0,\ t\notin[t_1,t_2] \Rightarrow \mathscr{C}_{\mathbf{H}}(t,f;\tau,\nu)=0,\ t\notin[t_1,t_2]$ |
| | $h^{(\mathrm{s})}(t,\tau)=0,\ \tau\notin[\tau_1,\tau_2] \Rightarrow \mathscr{C}_{\mathbf{H}}(t,f;\tau,\nu)=0,\ \tau\notin[\tau_1,\tau_2]$ |
| | $H^{(\mathrm{s})}(f,\nu)=0,\ f\notin[f_1,f_2] \Rightarrow \mathscr{C}_{\mathbf{H}}(t,f;\tau,\nu)=0,\ f\notin[f_1,f_2]$ |
| | $H^{(\mathrm{s})}(f,\nu)=0,\ \nu\notin[\nu_1,\nu_2] \Rightarrow \mathscr{C}_{\mathbf{H}}(t,f;\tau,\nu)=0,\ \nu\notin[\nu_1,\nu_2]$ |
| Symplectic covariance | $\tilde{\mathbf{H}} = \mu(\boldsymbol{A})\mathbf{H}\mu(\boldsymbol{A})^{+} \Rightarrow \mathscr{C}_{\tilde{\mathbf{H}}}(t,f;\tau,\nu) = \mathscr{C}_{\mathbf{H}}(\boldsymbol{A}\binom{t}{f};\boldsymbol{A}^{-1}\binom{\tau}{\nu})$ |

An estimate of the local scattering function was obtained by applying a nonstationary 2-D multiwindow estimator to a single measurement of the channel transfer function [45]. The results are shown in Fig. 6 for $f = f_c$ (the carrier frequency) and four different time instants corresponding to four different mobile positions. For $t = 5$ s (see Fig. 6(a)), there is no line-of-sight so that shadowing causes a large path loss. Furthermore, the Doppler frequencies close to $\nu_{\max} = 9.56$ Hz indicate that the angle of arrival (AOA) of all paths is about 0° (i.e., the waves arrive from ahead of the mobile). As the mobile approaches the corner, the delays gradually drift from $\tau = 0.5$ to 0.3 μs and the frequency spread of the Doppler components grows since the scatterer's angular spread and thus the AOA spread increase (see Fig. 6(b)). At about $t = 25$ s, the mobile passes the corner. This results in a strong line-of-sight component from broadside (AOA 90°, Doppler frequency ≈ 0 Hz) that can be seen in Fig. 6(c). At about $t = 40$ s, the mobile turned right which resulted in an AOA of ≈ 0° for the line-of-sight component and thus a dominant Doppler frequency $\approx \nu_{\max}$ (see Fig. 6(d)). A second, weaker contribution with Doppler frequency $\approx -\nu_{\max}$, i.e., AOA 180°, is due to a building located behind the mobile at that time.

## 6. Linear signal spaces

The success of the WD as a tool for analyzing deterministic signals suggested the definition of similar TF representations for collections of signals like *linear signal spaces* (discussed in this section) and *frames* (discussed in Section 7). A linear signal space $\mathscr{X}$ is a set of signals such that $c_1x_1(t) + c_2x_2(t) \in \mathscr{X}$ for any two elements $x_1(t), x_2(t) \in \mathscr{X}$ [55]. The signal space $\mathscr{X}$ can be characterized by a (nonunique) orthonormal basis or by the associated orthogonal projection operator [8] $\mathbf{P}_{\mathscr{X}}$. The dimension $N_{\mathscr{X}}$ of the space $\mathscr{X}$ equals the cardinality of any orthonormal basis spanning $\mathscr{X}$ or, equivalently, the rank of the projection operator $\mathbf{P}_{\mathscr{X}}$.

Using an arbitrary orthonormal basis $\{x_k(t)\}_{k\in\{1,\ldots,N_{\mathscr{X}}\}}$ of $\mathscr{X}$, the orthogonal projection

[8] The orthogonal projection operator $\mathbf{P}_{\mathscr{X}}$ associated to a signal space $\mathscr{X}$ is the self-adjoint ($\mathbf{P}_{\mathscr{X}}^{+} = \mathbf{P}_{\mathscr{X}}$) and idempotent ($\mathbf{P}_{\mathscr{X}}^{2} = \mathbf{P}_{\mathscr{X}}$) linear operator with range $\mathscr{X}$.

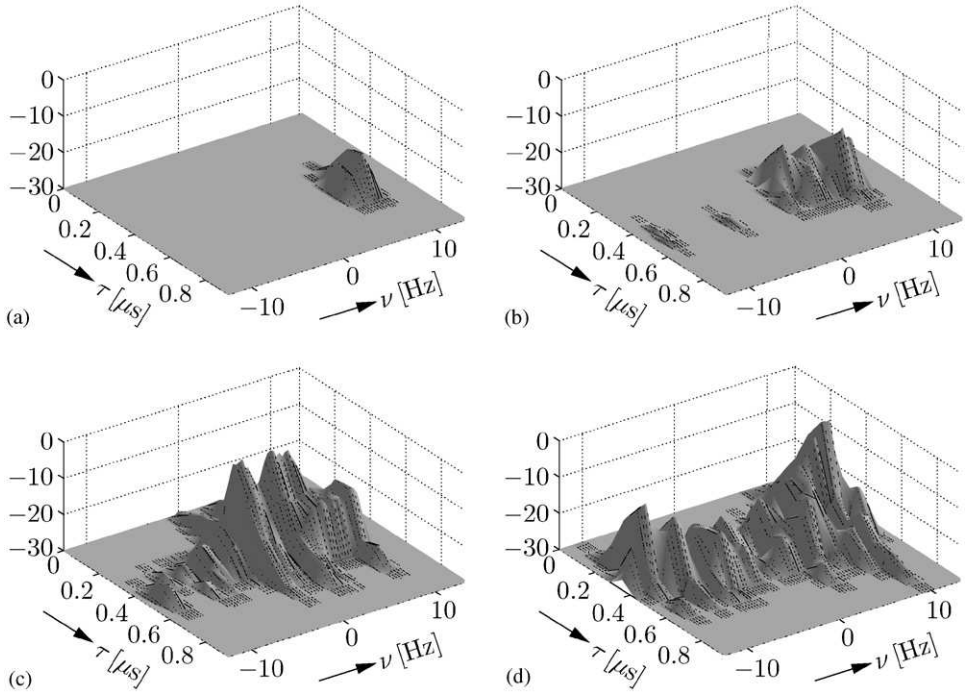


Fig. 6. Estimated local scattering function $\mathscr{C}_{\mathbf{H}}(t,f;\tau,\nu)$ (in dB) of a measured channel for $f=f_c$ and (a) $t=5$ s, (b) $t=20$ s, (c) $t=28$ s, (d) $t=40$ s.

operator can be written as

$$\mathbf{P}_{\mathscr{X}}=\sum_{k=1}^{N_{\mathscr{X}}} x_k\otimes x_k^*, \tag{21}$$

with kernel $p_{\mathscr{X}}(t,t')=\sum_{k=1}^{N_{\mathscr{X}}} x_k(t)x_k^*(t')$ (here, $x_k\otimes x_k^*$ is the rank-one projection operator on the one-dimensional space spanned by $x_k(t)$). Since the WD $W_{x_k}(t,f)$ characterizes the TF location of the energy of $x_k(t)$, it is reasonable to define the *WD of the signal space* $\mathscr{X}$ as the sum of all $W_{x_k}(t,f)$ [22,26], similar to (21):

$$W_{\mathscr{X}}(t,f)\triangleq\sum_{k=1}^{N_{\mathscr{X}}} W_{x_k}(t,f)$$

$$=\sum_{k=1}^{N_{\mathscr{X}}}\int_\tau x_k\left(t+\frac{\tau}{2}\right)x_k^*\left(t-\frac{\tau}{2}\right)\mathrm{e}^{-\mathrm{j}2\pi f\tau}\,\mathrm{d}\tau. \tag{22}$$

As will be made clear presently, the WD of $\mathscr{X}$ does not depend on the specific basis $\{x_k(t)\}$ used in the above definition. Eq. (22) suggests that $W_{\mathscr{X}}(t,f)$ describes the TF location of the signal space $\mathscr{X}$ in the sense that any signal $x(t)\in\mathscr{X}$ will be located in the TF region where $W_{\mathscr{X}}(t,f)$ is effectively nonzero. Signals located entirely in TF regions where $W_{\mathscr{X}}(t,f)\approx 0$ will be approximately orthogonal to $\mathscr{X}$.

For a one-dimensional space spanned by some signal $x(t)$, the WD of the space is just the WD of the signal (up to a scaling with the energy $\|x\|^2$ of the signal),

$$\mathscr{X}=\mathrm{span}\{x(t)\}$$

$$\Leftrightarrow\quad W_{\mathscr{X}}(t,f)=\frac{1}{\|x\|^2}W_x(t,f).$$

On the other hand, if $\mathscr{X}$ equals the space $L_2(\mathbb{R})$ of square-integrable signals then $W_{\mathscr{X}}(t,f)\equiv 1$, which means that $L_2(\mathbb{R})$ covers the entire TF plane. In fact, it can be shown that (at least for "nonsophisticated" spaces [22]) the WD of a space approximately equals 1 within the TF region where the signals contained in

Table 8
Some properties of the WD of a signal space

| | |
|---|---|
| TF shift covariance | $\widetilde{\mathscr{X}} = \mathbf{S}_{t_0,f_0}\mathscr{X} \Rightarrow W_{\widetilde{\mathscr{X}}}(t,f) = W_{\mathscr{X}}(t-t_0, f-f_0)$ |
| Realvaluedness | $W_{\mathscr{X}}(t,f) = W^*_{\mathscr{X}}(t,f)$ |
| Marginal properties | $\int_t W_{\mathscr{X}}(t,f)\,\mathrm{d}t = P_{\mathscr{X}}(f,f)$, $\int_f W_{\mathscr{X}}(t,f)\,\mathrm{d}f = p_{\mathscr{X}}(t,t)$ |
| Trace and energy | $\int_t\int_f W_{\mathscr{X}}(t,f)\,\mathrm{d}t\,\mathrm{d}f = N_{\mathscr{X}}$, $\int_t\int_f W^2_{\mathscr{X}}(t,f)\,\mathrm{d}t\,\mathrm{d}f = N_{\mathscr{X}}$ |
| Moyal-type relations | $\int_t\int_f W_{\mathscr{X}}(t,f)W_{\mathscr{Y}}(t,f)\,\mathrm{d}t\,\mathrm{d}f = \langle \mathbf{P}_{\mathscr{X}}, \mathbf{P}_{\mathscr{Y}}\rangle$ |
| | $\mathscr{X} \perp \mathscr{Y} \Rightarrow \int_t\int_f W_{\mathscr{X}}(t,f)W_{\mathscr{Y}}(t,f)\,\mathrm{d}t\,\mathrm{d}f = 0$ |
| | $\mathscr{X} \subseteq \mathscr{Y} \Rightarrow \int_t\int_f W_{\mathscr{X}}(t,f)W_{\mathscr{Y}}(t,f)\,\mathrm{d}t\,\mathrm{d}f = N_{\mathscr{X}}$ |
| Finite support | $\forall x(t)\in\mathscr{X}\colon x(t)=0,\ t\notin[t_1,t_2] \Rightarrow W_{\mathscr{X}}(t,f)=0,\ t\notin[t_1,t_2]$ |
| | $\forall x(t)\in\mathscr{X}\colon X(f)=0,\ f\notin[f_1,f_2] \Rightarrow W_{\mathscr{X}}(t,f)=0,\ f\notin[f_1,f_2]$ |
| Symplectic covariance | $\widetilde{\mathscr{X}} = \mu(\boldsymbol{A})\mathscr{X} \Rightarrow W_{\widetilde{\mathscr{X}}}(t,f) = W_{\mathscr{X}}(\boldsymbol{A}\binom{t}{f})$ |

$\mathscr{X}$ are located and 0 otherwise, i.e., $W_{\mathscr{X}}(t,f)$ is approximately the indicator function of a TF region $\mathscr{R}$ associated to $\mathscr{X}$. A relation supporting this interpretation is

$$0 \leqslant W_{\mathscr{X}}(t,f) *_t *_f W_w(-t,-f) = \|\mathbf{P}_{\mathscr{X}} w_{t,f}\|^2 \leqslant 1, \tag{23}$$

where $w(t)$ is an arbitrary normalized test signal. If the TF shifted signal $w_{t_0,f_0}(t)$ lies (mostly) within $\mathscr{X}$, then $\|\mathbf{P}_{\mathscr{X}} w_{t_0,f_0}\|^2 \approx 1$ and (23) shows that the local average of $W_{\mathscr{X}}(t,f)$ about the TF analysis point $(t_0,f_0)$ approximately equals 1. Conversely, if $w_{t_0,f_0}(t)$ lies mostly outside $\mathscr{X}$ (i.e., if $w_{t_0,f_0}(t)$ is effectively orthogonal to $\mathscr{X}$), then $\|\mathbf{P}_{\mathscr{X}} w_{t_0,f_0}\|^2 \approx 0$ and the local average of $W_{\mathscr{X}}(t,f)$ about $(t_0,f_0)$ is approximately 0. This interpretation of the WD of a linear signal space provides the basis for the design of *TF projection filters* [22,27,50]. Some further properties of $W_{\mathscr{X}}(t,f)$ are summarized in Table 8.

Interchanging integration and summation in (22) and comparing with (21), it is seen that

$$W_{\mathscr{X}}(t,f) = L_{\mathbf{P}_{\mathscr{X}}}(t,f) = \int_\tau p_{\mathscr{X}}\left(t+\frac{\tau}{2}, t-\frac{\tau}{2}\right) \mathrm{e}^{-\mathrm{j}2\pi f\tau}\,\mathrm{d}\tau.$$

That is, the WD of the space $\mathscr{X}$ equals the WS of the orthogonal projection operator $\mathbf{P}_{\mathscr{X}}$. This shows that $W_{\mathscr{X}}(t,f)$ is indeed independent of the specific basis $\{x_k(t)\}$ used in the definition (22). Because orthogonal projection operators are idempotent and self-adjoint, $\mathbf{P}_{\mathscr{X}} = \mathbf{P}^2_{\mathscr{X}} = \mathbf{P}^+_{\mathscr{X}}\mathbf{P}_{\mathscr{X}} = \mathbf{P}_{\mathscr{X}}\mathbf{P}^+_{\mathscr{X}}$, and thus (cf. (15) with $\mathbf{H}$ replaced by $\mathbf{P}_{\mathscr{X}}$)

$$W_{\mathscr{X}}(t,f) = W^{(\mathrm{I})}_{\mathbf{P}_{\mathscr{X}}}(t,f) = W^{(\mathrm{O})}_{\mathbf{P}_{\mathscr{X}}}(t,f).$$

That is, the WD of the space $\mathscr{X}$ equals the IWD/OWD of the projection operator $\mathbf{P}_{\mathscr{X}}$.

**Example.** We consider spaces spanned by $N_{\mathscr{X}}$ time-shifted versions of the ideally bandlimited sinc function $x_0(t) = \sin(\pi Bt)/(\pi\sqrt{B}t)$, i.e., $x_k(t) = x_0(t - k/B)$, $k = 1,\ldots,N_{\mathscr{X}}$. Fig. 7 shows the WD of such spaces for $N_{\mathscr{X}} = 1$, $N_{\mathscr{X}} = 12$, $N_{\mathscr{X}} = 24$, and $N_{\mathscr{X}} = 36$. In all four cases, the WD correctly reflects the bandlimitation of these signal spaces and its effective time support is an interval of duration $N_{\mathscr{X}}/B$. Within its effective TF support region of bandwidth $B$ and duration $N_{\mathscr{X}}/B$, the WD approximately equals 1, whereas outside this region the WD is approximately zero. Thus, the WD correctly indicates the TF support of the spaces. Note that the area of the effective TF support region equals the space dimension $N_{\mathscr{X}}$.

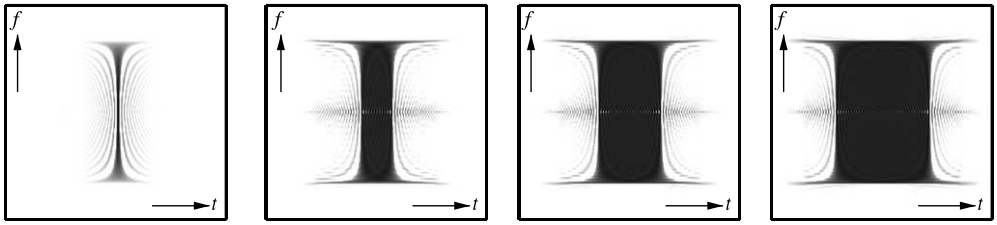


Fig. 7. WD of four signal spaces spanned by $N_{\mathscr{X}}$ time-shifted sinc functions with (a) $N_{\mathscr{X}}=1$, (b) $N_{\mathscr{X}}=12$, (c) $N_{\mathscr{X}}=24$, and (d) $N_{\mathscr{X}}=36$.

## 7. Frames

In recent years, nonorthogonal and, possibly, redundant (overcomplete) signal expansions have gained increasing popularity [14,15,21]. Examples include Gabor and wavelet expansions. The theory of *frames* [14,15,21] yields a powerful and convenient mathematical framework for the analysis and implementation of nonorthogonal signal expansions.

*Brief review of frame theory*. Consider a signal space (Hilbert space) $\mathscr{X}$. A set of functions $\mathscr{G}=\{g_k(t)\}$ with $g_k(t)\in\mathscr{X}$ is called a *frame* for $\mathscr{X}$ if

$$0<A\|x\|^2\leqslant\sum_k|\langle x,g_k\rangle|^2\leqslant B\|x\|^2<\infty \tag{24}$$

for every nonzero signal $x(t)\in\mathscr{X}$ (note that the $g_k(t)$ need not be orthogonal and the cardinality of $\mathscr{G}$ may be larger than the dimension of $\mathscr{X}$). The constants $A$ and $B$ are called *frame bounds*.[9] The *frame operator* $\mathbf{G}$ associated to $\mathscr{G}$ and its kernel are given by

$$\mathbf{G}=\sum_k g_k\otimes g_k^*,\qquad G(t,t')=\sum_k g_k(t)g_k^*(t') \tag{25}$$

(note the formal similarity to (21)). On $\mathscr{X}$, $\mathbf{G}$ is a self-adjoint, positive definite, invertible linear operator; furthermore, the lower and upper frame bounds equal the infimum and supremum, respectively, of the eigenvalues of $\mathbf{G}$.

The *dual frame* is the set of functions $\widetilde{\mathscr{G}}=\{\gamma_k(t)\}$ obtained as

$$\gamma_k(t)=(\mathbf{G}^{-1}g_k)(t),$$

where $\mathbf{G}^{-1}$ is the inverse frame operator. For the dual frame, the frame bounds are $A'=1/B$ and $B'=1/A$ and the frame operator equals $\mathbf{\Gamma}=\sum_k\gamma_k\otimes\gamma_k^*=\mathbf{G}^{-1}$. Using the frame $\mathscr{G}$ and the dual frame $\widetilde{\mathscr{G}}$, any signal $x(t)\in\mathscr{X}$ can be expanded as

$$x(t)=\sum_k\langle x,\gamma_k\rangle g_k(t)=\sum_k\langle x,g_k\rangle\gamma_k(t). \tag{26}$$

Thus, both $\mathscr{G}$ and $\widetilde{\mathscr{G}}$ span the signal space $\mathscr{X}$.

A frame is called *tight* if $A=B$. Here, $\mathbf{G}=A\mathbf{P}_{\mathscr{X}}$, where $\mathbf{P}_{\mathscr{X}}$ is the orthogonal projection operator on $\mathscr{X}$, and $\gamma_k(t)=g_k(t)/A$. An *orthonormal basis* is a special case of a tight frame with $A=B=1$. A frame with $A\approx B$ is called *snug*. Snug frames are desirable since here $g_k(t)\approx\gamma_k(t)$. Furthermore, frame bounds that are close to each other entail numerical stability of the expansions (26).

*The WD of a frame*. It is possible to establish a TF analysis of frames using a similar approach as for linear signal spaces (cf. Section 6). Since the WD $W_{g_k}(t,f)$ of an individual frame function $g_k(t)$ characterizes the TF location of the energy of $g_k(t)$, the *WD*[10] *of the frame* $\mathscr{G}$ can be defined as the sum of all $W_{g_k}(t,f)$ [23], similar to (25):

$$W_{\mathscr{G}}(t,f)\triangleq\sum_k W_{g_k}(t,f)$$

$$=\sum_k\int_\tau g_k\left(t+\frac{\tau}{2}\right)g_k^*\left(t-\frac{\tau}{2}\right)\mathrm{e}^{-\mathrm{j}2\pi f\tau}\,\mathrm{d}\tau. \tag{27}$$

[9] In what follows, we consider the largest possible $A$ and the smallest possible $B$.

[10] In [23], what we here call the WD of a frame was originally called the Weyl symbol of a frame, and the term "WD of a frame" was used for the IWD/OWD of the frame operator.

Table 9
Some properties of the WD of a frame

| | |
|---|---|
| TF shift covariance | $\widetilde{\mathscr{G}} = \mathbf{S}_{t_0,f_0}\mathscr{G} \Rightarrow W_{\widetilde{\mathscr{G}}}(t,f) = W_{\mathscr{G}}(t-t_0, f-f_0)$ |
| Realvaluedness | $W_{\mathscr{G}}(t,f) = W^*_{\mathscr{G}}(t,f)$ |
| Marginal properties | $\int_t W_{\mathscr{G}}(t,f)\,\mathrm{d}t = \hat{G}(f,f),\ \int_f W_{\mathscr{G}}(t,f)\,\mathrm{d}f = G(t,t)$ |
| Trace | $AN_{\mathscr{X}} \leqslant \int_t\int_f W_{\mathscr{G}}(t,f)\,\mathrm{d}t\,\mathrm{d}f = \mathrm{tr}\{\mathbf{G}\} \leqslant BN_{\mathscr{X}}$ |
| Energy | $A^2N_{\mathscr{X}} \leqslant \int_t\int_f W^2_{\mathscr{G}}(t,f)\,\mathrm{d}t\,\mathrm{d}f = \|\mathbf{G}\|^2 \leqslant B^2N_{\mathscr{X}}$ |
| Moyal-type relation | $\int_t\int_f W_{\mathscr{G}_1}(t,f)W_{\mathscr{G}_2}(t,f)\,\mathrm{d}t\,\mathrm{d}f = \langle \mathbf{G}_1, \mathbf{G}_2\rangle$ |
| Finite support | $\forall k\colon g_k(t) = 0,\ t \notin [t_1,t_2] \Rightarrow W_{\mathscr{G}}(t,f) = 0,\ t \notin [t_1,t_2]$ |
| | $\forall k\colon G_k(f) = 0,\ f \notin [f_1,f_2] \Rightarrow W_{\mathscr{G}}(t,f) = 0,\ f \notin [f_1,f_2]$ |
| Symplectic covariance | $\widetilde{\mathscr{G}} = \mu(\boldsymbol{A})\mathscr{G} \Rightarrow W_{\widetilde{\mathscr{G}}}(t,f) = W_{\mathscr{G}}(\boldsymbol{A}\binom{t}{f})$ |

This definition suggests that $W_{\mathscr{G}}(t,f)$ describes the TF location of the frame $\mathscr{G}$ in the sense that any signal $x(t) \in \mathscr{X}$ will be located in the TF region where $W_{\mathscr{G}}(t,f)$ is effectively nonzero. Some basic properties of the WD of a frame are summarized in Table 9.

Again, local averages of the WD of a frame shed additional light on its interpretation. In particular, it can be shown that

$$A \leqslant W_{\mathscr{G}}(t,f) *_t *_f W_w(-t,-f) = \langle \mathbf{G}w_{t,f}, w_{t,f}\rangle \leqslant B, \tag{28}$$

where $w(t)$ is an arbitrary normalized signal. According to (28), (a local average of) the WD of the frame $\mathscr{G}$ correctly reflects the frame bounds $A$ and $B$. If $W_{\mathscr{G}}(t,f)$ consistently assumes low values in a TF region of area $\geqslant 1$ and high values in another TF region of area $\geqslant 1$, then (28) shows that the frame bounds must be widely different and thus the frame is not snug. Conversely, if $W_{\mathscr{G}}(t,f)$ is approximately constant over the TF region that corresponds to the space $\mathscr{X}$, then the frame will be snug. Finally, if $W_{\mathscr{G}}(t,f)$ is approximately constant in some TF region of area $\geqslant 1$, then the frame is "locally snug" on the subspace of $\mathscr{X}$ corresponding to that TF region [23]. Thus, the WD shows the TF dependence of a frame's snugness.

Interchanging integration and summation in (27) and comparing with (25), it is seen that

$$W_{\mathscr{G}}(t,f) = L_{\mathbf{G}}(t,f) = \int_\tau G\left(t+\frac{\tau}{2}, t-\frac{\tau}{2}\right)\mathrm{e}^{-\mathrm{j}2\pi f\tau}\,\mathrm{d}\tau.$$

That is, the WD of a frame $\mathscr{G}$ equals the WS of the frame operator $\mathbf{G}$. For a tight frame, one can show that

$$W_{\mathscr{G}}(t,f) = AW_{\mathscr{X}}(t,f),$$

where $W_{\mathscr{X}}(t,f)$ is the WD of the signal space $\mathscr{X}$ spanned by $\mathscr{G}$. For an orthonormal basis (or, more generally, any tight frame with $A=1$), there is $W_{\mathscr{G}}(t,f) = W_{\widetilde{\mathscr{G}}}(t,f) = W_{\mathscr{X}}(t,f)$. If $\mathscr{G}$ is a tight frame for $\mathscr{X} = L_2(\mathbb{R})$, then $W_{\mathscr{X}}(t,f) \equiv 1$ and thus $W_{\mathscr{G}}(t,f) \equiv A$, i.e., the WD of the frame is constant over the entire TF plane.

*Gabor frames.* A particularly interesting special case is given by *Gabor* or *Weyl-Heisenberg* frames [15,21]. These frames are obtained by TF shifting a window $g(t)$ to the TF points $(kT, lF)$ that define a TF lattice with lattice constants $T$ and $F$. That is, $\mathscr{G} = \{g_{k,l}(t)\}$ with $g_{k,l}(t) = (\mathbf{S}_{kT,lF}g)(t) = g(t-kT)\mathrm{e}^{\mathrm{j}2\pi lFt}$, $k,l \in \mathbb{Z}$. The dual frame of a Gabor frame is also a Gabor frame with dual window $\gamma(t) = (\mathbf{G}^{-1}g)(t)$. The WD

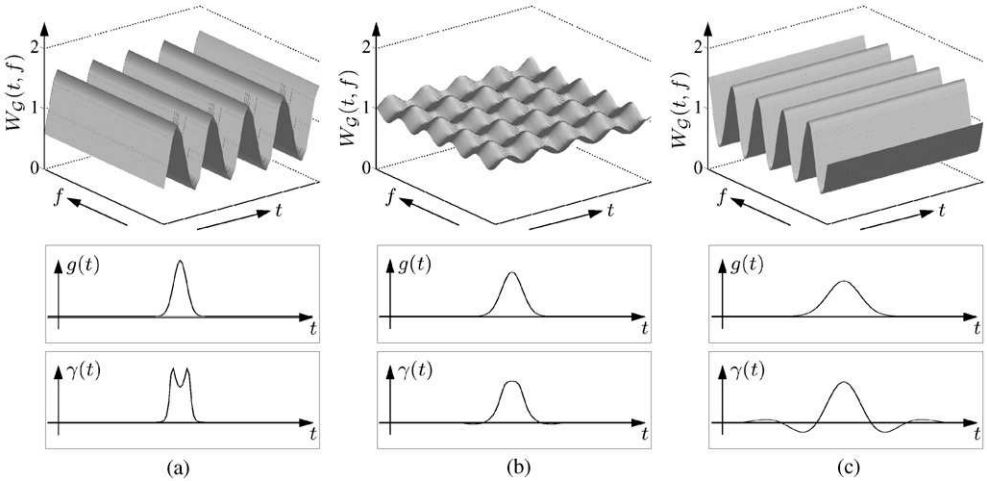


Fig. 8. WD (top), generating window $g(t)$ (center), and dual window $\gamma(t)$ (bottom) for three different Gabor frames with $TF = 1/2$. The window $g(t)$ is a Gaussian function of (a) short, (b) medium, and (c) large effective duration.

of a Gabor frame can be shown to equal

$$W_\mathcal{G}(t,f) = \sum_{k=-\infty}^{\infty} \sum_{l=-\infty}^{\infty} W_g(t-kT, f-lF),$$

which implies that $W_\mathcal{G}(t,f) = W_\mathcal{G}(t-T,f) = W_\mathcal{G}(t,f-F)$, i.e., $W_\mathcal{G}(t,f)$ is 2-D periodic.

We next restrict to $TF = 1/(2n)$, $n \in \mathbb{N}$. For this special case, it can be shown that

$$W_\mathcal{G}(t,f) = |Z_g(t,f)|^2. \tag{29}$$

Here,

$$Z_g(t,f) \triangleq \sqrt{T} \sum_{n=-\infty}^{\infty} g(t+nT)\mathrm{e}^{-\mathrm{j}2\pi nfT}$$

denotes the *Zak transform* of $g(t)$ [21,35] which is of fundamental importance in the theory of Gabor frames [15,21]. Based on (29), it can be shown that $W_\mathcal{G}(t,f)$ can be interpreted as the (continuous) eigenvalue distribution of the frame operator. As a consequence, one has

$$A = \min_{\substack{t\in[0,T]\\ f\in[0,F]}} W_\mathcal{G}(t,f),$$
$$B = \max_{\substack{t\in[0,T]\\ f\in[0,F]}} W_\mathcal{G}(t,f). \tag{30}$$

These relations can be viewed as sharp versions of the frame-bound inequalities in (28) (note that the restriction to the fundamental TF cell $[0,T]\times[0,F]$ in (30) is possible due to the periodicity of $W_\mathcal{G}(t,f)$).

**Example.** Fig. 8 shows the WD of three different Gabor frames with $TF = 1/2$, i.e., oversampling factor 2. The generating window $g(t)$ is chosen as the normalized Gaussian function $g(t) = (1/\sqrt{2^{1/2}T_g})\mathrm{e}^{-\pi(t/T_g)^2}$ with three different time constants $T_g$ corresponding to a "short," "medium," and "large" effective duration of the window. The WD in Fig. 8(a) features a strong variation in the time direction, which indicates that the window $g(t)$ is too short relative to $T$. Indeed, the ratio of the frame bounds determined according to (30) is $B/A = 3.7$, which means that the frame is far from being snug; the angle between $g(t)$ and $\gamma(t)$ is $\phi = \arccos\langle g,\gamma\rangle/(\|g\|\,\|\gamma\|) = 25.3°$. Similar observations apply to Fig. 8(c). Here, the WD features a strong variation in the frequency direction, which indicates that $g(t)$ is too narrowband or, equivalently, too long. In this case, $B/A = 3.4$ and $\phi = 24°$. In contrast, Fig. 8(b) shows that for the medium-duration window the WD of the associated frame is reasonably flat. Here, $B/A = 1.41$, i.e., the frame is quite snug. Indeed, in this case $\phi = 4.9°$, which means that $g(t)$ and $\gamma(t)$ are almost collinear.

## 8. Conclusion

We have discussed extensions of the Wigner distribution (WD) to multidimensional vector signals, nonstationary random processes, linear time-varying systems (both deterministic and random), linear signal spaces, and frames. All WD extensions we considered are based on the Weyl symbol (WS), which thus provides a unifying transformation or representation. Specifically,

- the ordinary WD of a signal is the WS of a rank-one operator,
- the Wigner–Ville spectrum (expected WD of a random process) is the WS of a correlation operator,
- the WD of a signal space is the WS of an orthogonal projection operator,
- and the WD of a frame is the WS of a frame operator.

We studied fundamental properties of the various WD extensions, and we pointed out numerous relations connecting them. We also illustrated by means of application examples how specific characteristics of a signal, system, random process, signal space, or frame can be inferred from its WD.

Our discussion has shown that the basic WD concept can be extended to several important domains beyond one-dimensional, scalar, deterministic signals. In each of these domains, the respective WD is a time–frequency representation that is both theoretically outstanding and practically useful.

## References

[1] M.J. Bastiaans, Application of the Wigner distribution function in optics, in: W. Mecklenbräuker, F. Hlawatsch (Eds.), The Wigner Distribution—Theory and Applications in Signal Processing, Elsevier, Amsterdam, The Netherlands, 1997, pp. 375–424.

[2] P.A. Bello, Characterization of randomly time-variant linear channels, IEEE Trans. Comm. Systems 11 (1963) 360–393.

[3] B. Boashash (Ed.), Time–Frequency Signal Analysis and Processing, Prentice-Hall, Englewood Cliffs, NJ, 2003.

[4] N.G. de Bruijn, A theory of generalized functions with applications to Wigner distribution and Weyl correspondence, Nieuw Arch. Wiskunde (3) XXI (1973) 205–280.

[5] S. Carstens-Behrens, M. Wagner, J.F. Böhme, Detection of multiple resonances in noise, Int. J. Electron. Comm. (AEÜ) 52 (5) (1998) 285–292.

[6] T.A.C.M. Claasen, W.F.G. Mecklenbräuker, The Wigner distribution—a tool for time–frequency signal analysis; Part I: continuous-time signals, Philips J. Res. 35 (3) (1980) 217–250.

[7] T.A.C.M. Claasen, W.F.G. Mecklenbräuker, The Wigner distribution—a tool for time–frequency signal analysis; Part II: discrete-time signals, Philips J. Res. 35 (4/5) (1980) 276–300.

[8] T.A.C.M. Claasen, W.F.G. Mecklenbräuker, The Wigner distribution—a tool for time–frequency signal analysis; Part III: relations with other time–frequency signal transformations, Philips J. Res. 35 (6) (1980) 372–389.

[9] T.A.C.M. Claasen, W.F.G. Mecklenbräuker, The aliasing problem in discrete-time Wigner distributions, IEEE Trans. Acoustics Speech Signal Process. 31 (5) (1983) 1067–1072.

[10] T.A.C.M. Claasen, W.F.G. Mecklenbräuker, On the time–frequency discrimination of energy distributions: can they look sharper than Heisenberg?, in: Proceedings of the IEEE ICASSP-84, San Diego, CA, 1984, pp. 41B7.1–41B7.4.

[11] L. Cohen, Time–Frequency Analysis, Prentice-Hall, Englewood Cliffs, NJ, 1995.

[12] H. Cramér, On some classes of nonstationary stochastic processes, in: Proceedings of the Fourth Berkeley Symposium on Mathematics, Statistics and Probability, University of California Press, CA, 1961, pp. 57–78.

[13] I. Daubechies, Time–frequency localization operators: a geometric phase space approach, IEEE Trans. Inform. Theory 34 (July 1988) 605–612.

[14] I. Daubechies, Ten Lectures on Wavelets, SIAM, Philadelphia, PA, 1992.

[15] H.G. Feichtinger, T. Strohmer (Eds.), Gabor Analysis and Algorithms: Theory and Applications, Birkhäuser, Boston, MA, 1998.

[16] P. Flandrin, A time–frequency formulation of optimum detection, IEEE Trans. Acoust. Speech Signal Process. 36 (9) (1988) 1377–1384.

[17] P. Flandrin, Time–Frequency/Time-Scale Analysis, Academic Press, San Diego, CA, 1999.

[18] P. Flandrin, W. Martin, The Wigner–Ville spectrum of nonstationary random signals, in: W. Mecklenbräuker, F. Hlawatsch (Eds.), The Wigner Distribution—Theory and Applications in Signal Processing, Elsevier, Amsterdam, The Netherlands, 1997, pp. 211–267.

[19] G.B. Folland, Harmonic Analysis in Phase Space, Annals of Mathematics Studies, Vol. 122, Princeton University Press, Princeton, NJ, 1989.

[20] G.B. Folland, A. Sitaram, The uncertainty principle: a mathematical survey, J. Fourier Anal. Appl. 3 (3) (1997) 207–238.

[21] K. Gröchenig, Foundations of Time–Frequency Analysis, Birkhäuser, Boston, 2001.

[22] F. Hlawatsch, Time–Frequency Analysis and Synthesis of Linear Signal Spaces: Time–Frequency Filters, Signal Detection and Estimation, and Range-Doppler Estimation, Kluwer, Boston, MA, 1998.

[23] F. Hlawatsch, H. Bölcskei, Time–frequency analysis of frames, in: Proceedings of the IEEE-SP International

Symposium on Time–Frequency and Time-Scale Analysis, Philadelphia, PA, October 1994, pp. 52–55.
[24] F. Hlawatsch, G.F. Boudreaux-Bartels, Linear and quadratic time–frequency signal representations, IEEE Signal Process. Mag. 9 (April 1992) 21–67.
[25] F. Hlawatsch, P. Flandrin, The interference structure of the Wigner distribution and related time–frequency signal representations, in: W. Mecklenbräuker, F. Hlawatsch (Eds.), The Wigner Distribution—Theory and Applications in Signal Processing, Elsevier, Amsterdam, The Netherlands, 1997, pp. 59–133.
[26] F. Hlawatsch, W. Kozek, The Wigner distribution of a linear signal space, IEEE Trans. Signal Process. 41 (March 1993) 1248–1258.
[27] F. Hlawatsch, W. Kozek, Time–frequency projection filters and time–frequency signal expansions, IEEE Trans. Signal Process. 42 (December 1994) 3321–3334.
[28] F. Hlawatsch, G. Matz, Time–frequency signal processing: a statistical perspective, in: Proceedings of the Workshop on Circuits, Systems and Signal Processing, Mierlo, The Netherlands, November 1998, pp. 207–219.
[29] F. Hlawatsch, G. Matz, Quadratic time–frequency analysis of linear time-varying systems, in: L. Debnath (Ed.), Wavelet Transforms and Time–Frequency Signal Analysis, Birkhäuser, Boston, MA, 2001, pp. 235–287 (Chapter 9).
[30] F. Hlawatsch, G. Matz, Time–frequency methods for nonstationary statistical signal processing, in: B. Boashash (Ed.), Time–Frequency Signal Analysis and Processing, Prentice-Hall, Englewood Cliffs, NJ, 2003.
[31] F. Hlawatsch, G. Matz, H. Kirchauer, W. Kozek, Time–frequency formulation, design, and implementation of time-varying optimal filters for signal estimation, IEEE Trans. Signal Process. 48 (May 2000) 1417–1432.
[32] F. Hlawatsch, T. Twaroch, H. Bölcskei, Wigner-type *a–b* and time–frequency analysis based on conjugate operators, in: Proceedings of the IEEE ICASSP-96, Atlanta, GA, May 1996, pp. 1395–1398.
[33] L. Hörmander, The Weyl calculus of pseudo-differential operators, Comm. Pure Appl. Math. 32 (1979) 359–443.
[34] http://www.nt.tuwien.ac.at/mobile/projects/METAMORP.
[35] A.J.E.M. Janssen, The Zak transform: a signal transform for sampled time-continuous signals, Philips J. Res. 43 (1) (1988) 23–69.
[36] A.J.E.M. Janssen, Positivity and spread of bilinear time–frequency distributions, in: W. Mecklenbräuker, F. Hlawatsch (Eds.), The Wigner Distribution—Theory and Applications in Signal Processing, Elsevier, Amsterdam, The Netherlands, 1997, pp. 1–58.
[37] D. König, J.F. Böhme, Application of cyclostationary and time–frequency signal analysis to car engine diagnosis, in: Proceedings of the IEEE ICASSP-94, Adelaide, Australia, April 1994, pp. 149–152.
[38] W. Kozek, Time–frequency signal processing based on the Wigner–Weyl framework, Signal Process. 29 (October 1992) 77–92.
[39] W. Kozek, On the underspread/overspread classification of nonstationary random processes, in: K. Kirchgässner, O. Mahrenholtz, R. Mennicken (Eds.), Proceedings of the International Conference on Industrial and Applied Mathematics, Mathematical Research, Vol. 3, Akademieverlag, Berlin, 1996, pp. 63–66.
[40] W. Kozek, On the transfer function calculus for underspread LTV channels, IEEE Trans. Signal Process. 45 (January 1997) 219–223.
[41] W. Kozek, F. Hlawatsch, H. Kirchauer, U. Trautwein, Correlative time–frequency analysis and classification of nonstationary random processes, in: Proceedings of the IEEE-SP International Symposium on Time–Frequency and Time-Scale Analysis, Philadelphia, PA, October 1994, pp. 417–420.
[42] B.V.K. Kumar, K.J. deVos, Linear system description using Wigner distribution functions, in: Proceedings of the SPIE, Advanced Algorithms and Architectures for Signal Processing II, Vol. 826, 1987, pp. 115–124.
[43] W. Martin, P. Flandrin, Wigner–Ville spectral analysis of nonstationary processes, IEEE Trans. Acoust. Speech Signal Process. 33 (December 1985) 1461–1470.
[44] G. Matz, A time–frequency calculus for time-varying systems and nonstationary processes with applications, Ph.D. Thesis, Vienna University of Technology, November 2000.
[45] G. Matz, Characterization of non-WSSUS fading dispersive channels, in: Proceedings of the IEEE ICC-2003, Anchorage, AS, May 2003.
[46] G. Matz, F. Hlawatsch, Time–frequency formulation and design of optimal detectors, in: Proceedings of the IEEE-SP International Symposium on Time–Frequency and Time-Scale Analysis, Paris, France, June 1996, pp. 213–216.
[47] G. Matz, F. Hlawatsch, Time–frequency transfer function calculus (symbolic calculus) of linear time-varying systems (linear operators) based on a generalized underspread theory, J. Math. Phys. (Special Issue on Wavelet and Time–Frequency Analysis) 39 (August 1998) 4041–4071.
[48] G. Matz, F. Hlawatsch, Time-varying spectra for underspread and overspread nonstationary processes, in: Proceedings of the 32nd Asilomar Conference on Signals, Systems, Computers, Pacific Grove, CA, November 1998, pp. 282–286.
[49] G. Matz, F. Hlawatsch, Time–frequency subspace detectors and application to knock detection, Int. J. Electron. Comm. (AEÜ) 53 (6) (1999) 379–385.
[50] G. Matz, F. Hlawatsch, Time–frequency projection filters: online implementation, subspace tracking, and application to interference suppression, in: Proceedings of the IEEE ICASSP-2002, Orlando, FL, May 2002, pp. 1213–1216.
[51] G. Matz, F. Hlawatsch, Linear time–frequency filters: online algorithms and applications, in: A. Papandreou-Suppappola (Ed.), Applications in Time–Frequency Signal Processing, CRC Press, Boca Raton, FL, 2002, pp. 205–271.
[52] G. Matz, F. Hlawatsch, Time–frequency characterization of random time-varying channels, in: B. Boashash (Ed.), Time–Frequency Signal Analysis and Processing, Prentice-Hall, Englewood Cliffs, NJ, 2003.
[53] W. Mecklenbräuker, A tutorial on non-parametric bilinear time–frequency signal representations, in: J.L. Lacoume, T.S. Durrani, R. Stora (Eds.), Traitement du Signal/Signal

Processing, Les Houches, Session XLV, Elsevier, Amsterdam, 1987, pp. 277–336.
[54] W. Mecklenbräuker, F. Hlawatsch (Eds.), The Wigner Distribution—Theory and Applications in Signal Processing, Elsevier, Amsterdam, The Netherlands, 1997.
[55] A.W. Naylor, G.R. Sell, Linear Operator Theory in Engineering and Science, 2nd Edition, Springer, New York, 1982.
[56] J.C. O'Neill, P. Flandrin, W.J. Williams, On the existence of discrete Wigner distributions, IEEE Signal Process. Lett. 6 (December 1999) 304–306.
[57] A. Papoulis, Probability, Random Variables, and Stochastic Processes, 3rd Edition, McGraw-Hill, New York, 1991.
[58] F. Peyrin, R. Prost, A unified definition for the discrete-time, discrete-frequency, and discrete-time/frequency Wigner distribution, IEEE Trans. Acoust. Speech Signal Process. 34 (August 1986) 858–867.
[59] J. Ramanathan, P. Topiwala, Time–frequency localization via the Weyl correspondence, SIAM J. Matrix Anal. Appl. 24 (5) (1993) 1378–1393.
[60] T.S. Rappaport, Wireless Communications: Principles & Practice, Prentice-Hall, Upper Saddle River, NJ, 1996.
[61] M.S. Richman, T.W. Parks, R.G. Shenoy, Discrete-time, discrete-frequency time–frequency analysis, IEEE Trans. Signal Process. 46 (June 1998) 1517–1527.
[62] A.M. Sayeed, D.L. Jones, Optimal detection using bilinear time–frequency and time-scale representations, IEEE Trans. Signal Process. 43 (December 1995) 2872–2883.
[63] R.G. Shenoy, T.W. Parks, The Weyl correspondence and time–frequency analysis, IEEE Trans. Signal Process. 42 (February 1994) 318–331.
[64] J. Ville, Théorie et applications de la notion de signal analytique, Câbles Transm. (2ème A) (1) (1948) 61–74.
[65] H. Weyl, The Theory of Groups and Quantum Mechanics, Dover Publications, New York, 1950.
[66] E.P. Wigner, On the quantum correction for thermodynamic equilibrium, Phys. Rev. 40 (June 1932) 749–759.
[67] M.W. Wong, Weyl Transforms, Springer, New York, 1998.
[68] Y. Zhang, M.G. Amin, Spatial averaging of time–frequency distributions for signal recovery in uniform linear arrays, IEEE Trans. Signal Process. 48 (10) (2000) 2892–2902.